The dynamic effect of rail joint on Railway Track components

By

Abraham Girma

Advisor

Mathias Kabtamu, Msc.,

A Thesis submitted to the school of Graduate studies of Addis Ababa University

In

Partial Fulfillment of the Requirements for the Degree of Masters of Science in

Civil Railway Engineering

June 2017

ADDIS ABABA UNIVERSITY

SCHOOL OF GRADUATE STUDIES

As member of the Examining Board of the final M.Sc, Open Defense, we certify that we have read and evaluated the thesis prepared by: **Abraham Girma**

Entitled: **The dynamic effect of rail joint on Railway Track components**

And recommended that it be accepted as fulfilling the thesis requirement for the Degree of Masters of Science in Civil Railway Engineering

SUBMITTED BY

Abraham Girma ______________ ______________

Signature Date

APPROVED BY

Ato Mathias Kabtamu _______________ ________________

Advisor Signature Date

Dr Birhanu Besha _______________ ________________

Chairman, Dept.'s Graduate Committee Signature Date

Ato Abdulsetar Siraj ____________________ ______________

Internal Examiner Signature Date

Ato Mequanent Mulugeta ___________________ _______________

External Examiner Signature Date

Certification

I, Abraham Girma, declare that this thesis, submitted in fulfillment of the requirements for the MSC in Railway Engineering, in the School of Civil and Environmental Engineering, University of Addis Ababa Institute of Technology, is wholly my own work unless otherwise referenced or acknowledged. The document has not been submitted for qualifications at any other academic institution.

Acknowledgement

First of all, I would like to thank my almighty God for the accomplishment of this thesis. Next to God, I would like to thank Mr. Mathias Kabtamu for all of his helpful advices and suggestions for my thesis. Then, I would like also to grateful Addis Ababa University Institute and of Technology and Ethiopian Railway Corporation for the golden opportunity giving to me to conduct this Masters of Railway Engineering program. I would also like to thanks my family for their support and encouragement during the time of my studies. And finally, I would like to thank my friends who have given me their time and their priceless support for the successful conducting of this thesis.

Addis Ababa, June 2017

Abraham Girma Haileselassie

Abstract

A rail irregularity is the weakest link in the railway track which highly creates the impact forces. The impact forces in the rail irregularity such as insulated rail joints or bolted rail joints can be extremely large and can cause serious failures in the track structure, which can lead to a significant economic loss for track owners by making damage to rails and to the sleepers beneath.

The main question that to be answered in relation to the imperfection or rail irregularity especially with the bolted jointed rail is that; "what is the dynamic effect of this weakest point or jointed rail on the railway track components". Thus, this paper is mainly focuses on the studying this effect. In analyzing this effect, the finite element modeling software, ABAQUS having 2D model algorithm is used to analyze the dynamic effect of the jointed rail on the track system response.

In doing this, four different vehicle speeds ranges from 60Km/hr to 200Km/hr are used for analyzing the dynamic effect of jointed rail on the railway track components. The results show that; as the vehicle speeds of the train increases from 60Km/hr to 200Km/hr, the spatial displacement of the rail, sleeper and ballast is also increases in zigzag forms for the entire length of the rail.

Apart from this, to further studying the dynamic effect of the jointed rail on the track components different type of rail pads having a stiffness of 50MN/m, 100MN/m, 150MN/m, 200MN/m and 500MN/m area also included in the study to account the dynamic effect of the rail pads on the track performance. The results this thesis indicates that; the rail pads stiffness has significant role in reducing the vertical vibration of the rail, sleeper and ballast.

Moreover, in order to further analyze the dynamic effect of the jointed rail on the railway track components; the effect of the position of sleepers, wheel load and diameters are also presented. In line with this, with all the above scenarios, the results show that as the vehicle speed of the wheel, wheel diameters and number of the wheels increases, the dynamic acceleration and spatial displacement of the rail, sleeper and ballast especially at and around the rail joints are also increases.

Further, the dynamic actions such as frequency analysis, acceleration and dynamic spatial displacement are also determined at and around the jointed rail. Thus, the vertical vibration of the rail and sleeper is maximum at the frequency range from 90Hz to 130Hz and the vertical vibration of the ballast is maximum at the frequency range from 174Hz to 300Hz.

Key words

Rail Joint, Dynamic analysis, Finite element modeling, frequency, spatial displacement, acceleration

Table of content Page

CERTIFICATION.. i

ACKNOWLEDGMENTS ii

ABSTRACT iii

TABLE OF CONTENTS iv

LIST OF FIGURES.. vii

LIST OF TABLES... ix

LIST OF SYMBOLS x

1. CHAPTER ONE INTRODUCTION 1

1.1 PROBLEM STATEMENT 3

1.2. OBJECTIVES 4

1.3 .SIGNIFICANCE OF RESEARCH 4

1.4 SCOPE OF RESEARCH 4

CHAPTER 2 LITERATURE REVIEW.. 6

2.1 BACK GROUND PHILOSOPHY OF IRREGULAR TRACK BEHAVIORS................................8

2.2 OVERVIEW OF RAIL JOINTS... .10

2.3 COMPONENT OF RAILWAY TRACK 12

2.4 TRACK MODELING 14

2.4.1 BEAM THEORIES 14

2.4.1.1 EULER-BERNOULLI BEAM (E-B BEAM) 14

2.4.1.2 RAYLEIGH- TIMOSHENKO BEAM (R-T BEAM).. 15

2.4.2 WINKLER FOUNDATION BEAM (RAIL) ON CONTINUOUS ELASTIC FOUNDATION…16

2.4.3 PASTERNAK FOUNDATION MODEL 16

2.4.4 DOUBLE LAYER BEAM MODELS 17

2.4.5 FINITE ELEMENT MODELLING USING ABAQUS 17

2.4.5.1 LINEAR EIGENVALUE ANALAYSIS 18

2.4.5.2 STEADY-STATE DYNAMIC ANALYSIS 18

2.4.5.3 IMPLICIT AND EXPLICIT DYANAMIC ANALYSIS 18

2.5 WHEEL RAIL CONTACT DYNAMICS 19

2.6 TRACK DYNAMICS OF RAIL JOINTS 20

2.6.1 TRACK CHARACTERISTICS 22

2.6.1.1 DYNAMICS EFFECTS 22

2.6.1.2 TRAIN SPEEDS 23

2.6.1.2 AXLE LOADS 23

2.6.2DYNAMIC PROPERTIES OF RAILPADS AND FASTENERS 23

2.6.3 DYNAMIC PROPERTIES OF SLEPPERS 24

2.6.4 DYNAMIC PROPERTIES OF BALLAST, SUBBALLAST AND SUBGRADE 24

CHAPTER 3 MODELLING AND MODELLING PARAMETERS 25

STRATEGY 1: SIMPLIFICATIONS OF GEOMETRY MODELING 25

3.1 BOUNDARY CONDITIONS........ 26

STRATEGY 2: SIMPLIFICATION OF MATERIAL MODELING 26

3. 2 DRUCKERS-PRAGER MODEL........ 27

STRATEGY-3: SIMPLIFICATION OF BOUNDARY CONDITIONS........ 28

STRATEGY-4: BOUNDARY CONDTIONS OF WHEEL........ 29

STRATEGY-5: WHEEL/RAIL CONTACT MODELING 31

CHAPTER 4 RESULLT AND DISCUSION 32

4.1: INTRODUCTION 32

4.2: RESULTS OF DYNAMIC ANALYSIS 32

4.2.1: NATURAL FREQUENCY ANALYSIS 32

4.2.2: THE DYNAMIC EXPLICIT ANALYSIS 43

CHAPTER 5 CONCLUSION AND RECOMMENDATION........ 65

5.1 CONCLUSION 65

5.2 RECOMMENDATIONS 67

REFERENCES 68

APPENDIX 71

List of Figures Page

Figure 2.1 Frequency diagram: coupling of wavelength *L* and speed *V* for typical wavelengths (short length-scales) in the train-track system. ……………………….……………………...….**9**

Figure 2.2 Assembled rail joint…………………………………………………...……...…**10**

Figure 2.3 Suspended rail joints and supported rail joints….……………………………………**11**

Figure 2.4 Types of Insulated Rail Joints……………………...…………………………...**11**

Figure 2-5: Components of railway track……………………………………………………..**12**

Figure 2.6: (a) Beam and applied force, (b) force acting on an element………………………...**14**

Figure 2.7 Pasternak foundation for beam ………………………...**17**

Figure 2.8 Dynamic force amplification in the case of rail joints…...…………………………**21**

Figure 3.1 Surface profile of real train wheel..……………………..**25**

Figure 3.2 Boundary conditions os wheel and rail joint……………………..........................**26**

Figure. 3.3 The rail support system……………………..**28**

Figure 3.4: Modeling……………………..……………………...…………………………**29**

Figure 3-5: Jointed rail……………………...………………………………………………**29**

Figure 3.6 The wheel Loading system……………………..**30**

Figure 4.1 the effect of Eigen frequency modes of vibration extracted for rail vertical deflection for 100 and 100 modes of extraction..**32**

Figure 4.2 Rail vertical displacement for the first 100 modes of vibration.................................**33**

Figure 4.3 Rail, sleeper and ballast vertical displacement for the first 1000 modes of vibration..**33**

Figure 4.4 Rail lateral displacements for the first 1000 modes of vibration................................**35**

Figure 4.5 Right rail lateral displacements...**35**

Figure 4.6 Left rail lateral displacement..**36**

Figure 4.7 Rails, sleeper and ballast vertical displacement...**36**

Figure 4.8 Rail to the left and right side of Jointed rail spatial Displacement.............................**40**

Figure 4.9 Frequency of the Left and Right sleeper……...**41**

Figure 4.10 Frequency of Ballast…..…...**42**

Figure 4.11 Acceleration of rail, sleeper and ballast as the vehicle moves from left to the right direction…………………………………………………………………………………**43**

Figure 4.12 Acceleration of rail, sleeper and ballast as the vehicle moving from right to the left direction……...**44**
Figure 4.13 Spatial displacement of rail, sleeper and ballast...**46**
Figure 4.14 Spatial displacement of the rail placed to the left side of rail join............................**47**
Figure 4.15 Spatial displacement of the rail placed to the right side of rail joint….......................**47**
Figure 4.16 Left rail Spatial displacement………...**48**
Figure 4.17 Right side sleeper spatial displacement……..**49**
Figure 4.18 Ballast spatial Displacement……………...**49**
Figure 4.19 The spatial displacement of rail, sleeper and ballast as the vehicle moves from right to the left……...**50**
Figure 4.20 the spatial displacement of rail, sleeper and ballast as the vehicle moves from the left to the right direction…..**51**
Figure 4.21 Right side jointed rail spatial displacement ………...**52**
Figure 4.22 Left side jointed rail spatial displacement ……………..**52**
Figure 4.23 Left side sleeper spatial displacement ……………..**53**
Figure 4.24 Right side sleeper spatial displacement ……………...**53**
Figure 4.25 Ballast spatial Displacement …………………...**54**
Figure 4.26 Rail spatial displacement ……………………...**55**
Figure 4.27 Suspended and Suppported Sleeper spatial displacement **56**
Figure 4.28 Suspended and Supported ballast spatial displacement **56**
Figure 4.29 left rail spatial displacement for different number of wheel …………….....................**57**
Figure 4.30 Right rail spatial displacements for different number of wheel................................**58**
Figure 4.31 Right sleeper spatial displacement...**58**
Figure 4.32 left sleeper spatial displacement...**59**
Figure 4.33 Ballast spatial displacement ………...**59**
Figure 4.34 Right rail spatial displacemnt for different wheel diameter......................................**60**
Figure 4.35 left rail spatial displacement for different wheel diameter.......................................**61**
Figure 4.36 Right sleeper spatial displacement for different wheel diameter..............................**61**
Figure 4.37 left sleeper spatial displacement for different wheel diameter………….....................**62**
Figure 4.38 Ballast spatial displacements for different wheel diameter.......................................**62**
Figure 4.39 Jointed bar Von misses stresses...**63**

Figure 4.40 Von misses Stresses of rail pad for the vehicle speed of 120Km/hr for different rail pad stiffness………..**64**

List of Tables Page

Table 3.1 Mechanical property of modeling material (AVE Zaragoza track) ….……….............**26**

Table 3.2 primary and secondary suspension stiffness and damping……………………….......**30**

Table 4.1 Frequency ranges for railway track vibration………………..………………………..**34**

List of Symbols

Mc	Car-body mass;
Ks2	Secondary suspension stiffness;
Cs2	Secondary suspension damping;
Mt	Bogie mass;
Jt:	Bogie pitch moment of inertia;
Ks1	Primary suspension stiffness;
Cs1	Primary suspension damping;
Mw	Wheel set mass;
E	Young's modulus;
I	Moment of inertia;
Kr	Rail-pad stiffness;
Cr	Rail-pad damping;
Ms	Sleeper mass;
(Φ_i)	Internal friction
(Φ_d)	Dilation angle
ϕ_p	Peak friction angle,
σ_1	Major principal stress
σ_3	Minor principal stress
q_{peak}	Maximum deviator stress.
EI	Bending stiffness
p	Density
A	Cross-sectional area
$q(x, t)$	Load
t	Time
$w(x, t)$	Deflection
$\psi\ (x, t)$	Shear deformation
G	Shear modulus
K	Shear factor

CHAPTER ONE

INTRODUCTION

A jointed rail is the weakest link in the track. There is a break in the continuity of the rail in horizontal as well as in vertical plane at this location because of the expansion gap and imperfection in the rail heads at joint. The impact forces in the rail irregularity such as insulated rail joints or bolted rail joints can be extremely large and can cause serious the failures in the track structure, which can lead to significant economic loss for track owners by making damage to rails and to the sleepers beneath.

When a train runs over a rail joint, large dynamic impact forces are developed which lead to vibrations in the structures and a higher probability of component fatigue and damage. Thus, this can cause serious failure in the track structure and as a result the effect of this rail joints can affect the maintenance costs, ride comfort and running security on a modern railway.

Track irregularities due to imperfect level and alignment will also cause oscillations or vibrations of the train, and this will induce discomfort for passengers and damage for goods. Consequently, the imperfection of the level and alignment that comes from jointed rail creates undulation of track and as result long and short wave length will be created through a long time. Subsequently, the long wavelength of the undulations of the track will give rise to low-frequency oscillations of the train and short wavelength irregularities of the track cause vibrations and noise both in the train and in the environment.

In connection with, the dynamic effect of the rail joint first create wear on the interfaces between rail and joint bar and after that, it causes loss of bolt tension and necessitates regular tightening of the nuts bending stiffness in the rail. Since the rail acts as a beam to distribute wheel loads over several crossties, a point of low rail stiffness tends to concentrate loads on the ties near that point. The increased deflection at the joint may also contribute to the development of low-frequency dynamic loads, as wheels move down at the joint and then back up to the normal loaded elevation of the rail. This effect will be magnified if the increased tie loads lead to greater settlement or loss of elastic stiffness in the ballast and subgrade under the joint. Finally, the small gap between one rail and the others create high-frequency impact loads as wheels pass over it.

Thus, it is required to clearly study the dynamic effect of the rail joint on the track components for taking the remedial measure for the undulations of the track that has been caused as result of the rail joints and as well as to further study it's consequence since it require extensive maintenance cost. Moreover, it is necessary that studying the dynamic effect of the rail joint on the railway track components is highly necessary for to examining its maintenance mechanism.

In this regards, the dynamic effect of the rail joints has been analyzed and examined in this study using finite element solver program known as Abaqus. Consequently, the result of the dynamic acceleration, spatial displacement and frequency analysis of the jointed rail on the railway track component is examined and analyzed. Furthermore, the result of the response of the jointed rail is more examined and analyzed by using different scenarios such as by varying the vehicle speed of the train, by using different rails pads stiffness, wheel diameter, and by varying the position of the rail joint that has been placed on the sleeper or between the sleepers.

1.1 Problem statement

Jointed rail are regarded as points of weakness in rail track network. The discontinuities induced by the rail joint to the rail, produce high frequency dynamic impact forces and as result it cause localized damage and failure on the track. This mechanism of failure is believed to cause significant reduction to service lives with subsequent increasing demand for maintenance to ensure safety. Subsequently, the reduction of the services life of track will be critical especially in heavy haul lines since the applied load on the railway track is higher in case of heavy haul lines.

Furthermore, currently the failure of the railway track is mainly observed at the jointed rail; thus, it is required to technically examine the dynamic effect of the jointed rail on the railway track components using the modeling software or by taking site experiment test. In connection with this, since the railway technology in our countries is not highly popular, thus, studying of the dynamic effect of the jointed rail on the railway track components using the software modeling is more preferable than the site experimental test.

Thus, in this study the dynamic effect of rail joint on railway track components is examined and analyzed by using the modeling software known as ABAQUS. Consequently, to prepare the capable jointed rail that has an ability to absorb the dynamic load of the track, studying of the dynamic effect of the jointed rail on the railway track components is more important. Therefore, in this thesis, the dynamic effect of the jointed rail on the railway track components has been studied and analyzed.

1.2 Objectives

The main objective of this thesis is mainly focuses on studying of the dynamic effect of jointed track using Finite element analysis and modeling software (ABAQUS).

With this in mind the following specific objectives can be drawn:

- To analyze the dynamic response of jointed rail such as dynamic spatial displacement, acceleration and track frequency analysis.
- To further analyze the dynamic effect of jointed rail on the railway track components using varying vehicle speed, rail pads stiffness, wheel diameter, number of the wheel for modeling and position of the sleepers placed under the rail.

1.3 Significance of research

It is known that studying of the dynamic effect of the jointed rail is paramount for minimizing the huge cost budgeted for the remedial measure or maintenance of the tracks. Thus, in order to take the remedial measure for the dynamic effect of the rail joints, studying of its effect is highly necessary. So, this thesis is prepared for studying this dynamic effect. Hence, based on the result obtained from this study, the improving mechanism for the frequent problems observed on the jointed rail will be easily determined. Even though now days the jointed rail is replaced by continuously welded track, the research output indicates that still the applicability of the jointed rail can be an option especially around small and medium haul line. Therefore, for the Ethiopian situation in which the most of the track is constructed using bolted jointed rail, studying the dynamic effect of the jointed rail is highly applicable.

Moreover, based on the result obtained from this study the upcoming Ethiopian researchers can develop a cost effective ways of minimizing the maintenance cost of jointed rail.

1.4 Scope of research

The scope of this research is to investigate the vibrational modes, acceleration and deflection excited by jointed rail.

In this regards, owing to the complexity of the modeling involved in the investigation of the wheel/rail contact-impact on the railhead in the vicinity of the rail end joint; the wear and defects on either the railhead or the wheel tread, railway track misalignments, Curved track, Longitudinal stress resulting from temperature fluctuations, Looseness of bolts, fasteners, Wagon/bogie/wheel set dynamics are considered as out of the scope of this research.

CHAPTER TWO

LITERATURE REVIEW

Introduction

When a train runs over a joint, large dynamic impact forces are developed which lead to vibrations in the structures and a higher probability of component fatigue and damage.

The impact forces in the rail irregularity such as insulated rail joints or bolted rail joints can be extremely large and can cause serious failures in the track structure, which can lead to significant economic loss for track owners through damage to rails and to the sleepers beneath. The wheel rail impact forces can be occurred by different reason. For example, it can be occurred by the imperfections in the wheel or rails such as wheel defects, rail defects, welded joints and bolted rail joints. These situations can cause the wheel-sets impact onto the track, thereby causing an impact force and a forced vibration with high frequencies.

Simply increasing the weight of rail, which creates greater stiffness or bending resistance, will not necessarily compensate for other poor components (e.g., sleepers or ballast). The system integration for a higher performance and long term structural usage depends on the system ability capable of resisting and/or transferring all types of loads acting. The system generally comprising of the vehicle, track and contact subsystems. Each subsystem again has its own components. [19]

The track and the train vehicle subsystems, from dynamic point of view, are coupled subsystems as an integral entity vibrating at the wheel-rail contact which is their common source of vibration, but mechanically, the two systems are separate in spite the train is moving on the track. Severe dynamic disturbances at the wheel-rail interface occur when geometric irregularities exist, either along the rail head surface-such as rail joints, imperfect rail welds and rail corrugations, or around the wheel circumference-such as wheel shells, flat spots, or a completely out-of-round wheel.

The jointed rail tracks are source of high-frequency excitations of both the track and the vehicle, especially, the higher the speed of trains and the higher effects of this irregularity increase the acceleration and deflection of the rail.

With respect to the track, high-frequency excitations are most detrimental for concrete sleepers, rail fastenings, and other track components and responsible for non-uniform ballast settlement or local decomposition under the irregularity section. Concerning the vehicle, high frequency excitations may introduce non-linearities in wheel–rail contact, causing non-continuous railhead damage and wheel flats. These high-frequency excitations finally lose their energy by dissipation (plastic deformation, irreversible creep, and other processes related to the growth of track damage) and migration to lower frequency vibrations of other train and track components. From the above point of view, it is crucial to realize a vertical rail joint geometry.[24]

In connection with this, many researchers has studied the dynamic behavior of the railway track using the rail with defect-free surfaces and defect surface. For continuous rails with defect-free surfaces, various studies have identified that the dynamic load factor (DLF) is affected by various parameters such as: the operating speed, the wheel diameter and the track condition parameter. [13, 14, 15] Rail tracks are generally designed using an equivalent dynamic load that is calculated by multiplying the static wheel load by the dynamic load factor. There are many formulae that define the dynamic load factor as a function of the track condition, operating speed and wheel load. [16, 17, 18] these formulae were typically developed to account for the large geometric deviations from the original design position that a track develops over its lifetime; typically the dynamic load factor varies between 1.05 and 2.45. [10]

Similarly, for the wheel-rail defect surface, the recent year's researchers have focused on the exploration of dynamic impact forces induced by wheel–rail defects. A number of models have been developed based on theoretical and traditional methods such as Beam on Elastic Foundation (BOEF) in the analysis [20,21] and on other alternative method such as the finite element method (FEM). Researchers have developed a number of finite element (FE) models for railway track force analyses, such as a wheel–rail system for different heights at a rail joint [22].

The ultimate result of all the researchers indicates that the irregularity of the wheel/rail interaction is the production of large wheel/rail impact forces, which are the principal cause of damage to the wheels, rails, and the track foundation. The formation and development of wheel/rail irregularities and the intensity of dynamic wheel/rail interaction are mutually responsible, each being the casualty of the other. The existence of a defective spot, either on the wheel circumference or on the rail surface, gives rise to wheel impact force on the rail, which in turn, causes the existing defect to grow and may initiate other types of irregularities on the wheel or rail surfaces-resulting in a 'vicious circle'. An adequate understanding of the mechanisms of these aspects of the wheel/rail and track interactive system is essential to formulate effective strategies to reduce or eliminate the adversities of the vehicle/track system. [11][12][23]

2.1 Back ground Philosophy of irregular Track behaviors

In general when the train passes rail joints, the track components starts vibrating. The running and simultaneously vibrating train causes fluctuating vertical track forces with different frequency components along the track. This causes the longer-wave irregularities to grow into the track. The above process can be illustrated through the simple case of rail joint with bolts. The – initially straight – joint is loaded by a passing axle. This causes the joint to deflect. This, on its turn, causes a nonzero dynamic axle load component. The result is a local settlement of the ballast bed after some time.

The vibrations, with different frequency components, which also depend on the actual train speed, lead to varying vertical track forces along the track, which induce non-uniform settlements. This is an explosively worsening situation of track deterioration. This example clearly illustrates how long-wave track irregularities start growing from local short-wave geometrical defects. Fig. 2.1 shows the relationship between typical wavelengths of some physical or geometrical in homogeneities which are present in the railway system and the resulting excitation frequencies as a function of the train speed. Further, the frequency area where significant dynamic amplification in the vehicle-track interaction is mainly of interest as well as the area in which vibration hindrance and train comfort are of main interest is indicated.
In the first area, which is obviously related to the short-wave regime of track irregularities, also the phenomena of structural damage to the train-track system and progressive track deterioration

enter. This can be easily explained by the fact that the energy of the high-frequency vibrations and waves is absorbed and dissipated in the components of the train-track system. The low-frequency vibrations and long waves cannot be easily absorbed by structural components; they therefore determine the dynamic behavior of the train and are radiated from the system into the environment. A clear transition between both frequency regimes does not exist, but the aim of Fig. 2.1 is to illustrate a general trend as well as the role of the short-wave contribution in the track geometry spectrum. This implies that the short-wave contribution of the spectrum of the track geometry must be taken into consideration in an effective track assessment, such as pointed out in e.g. [30].

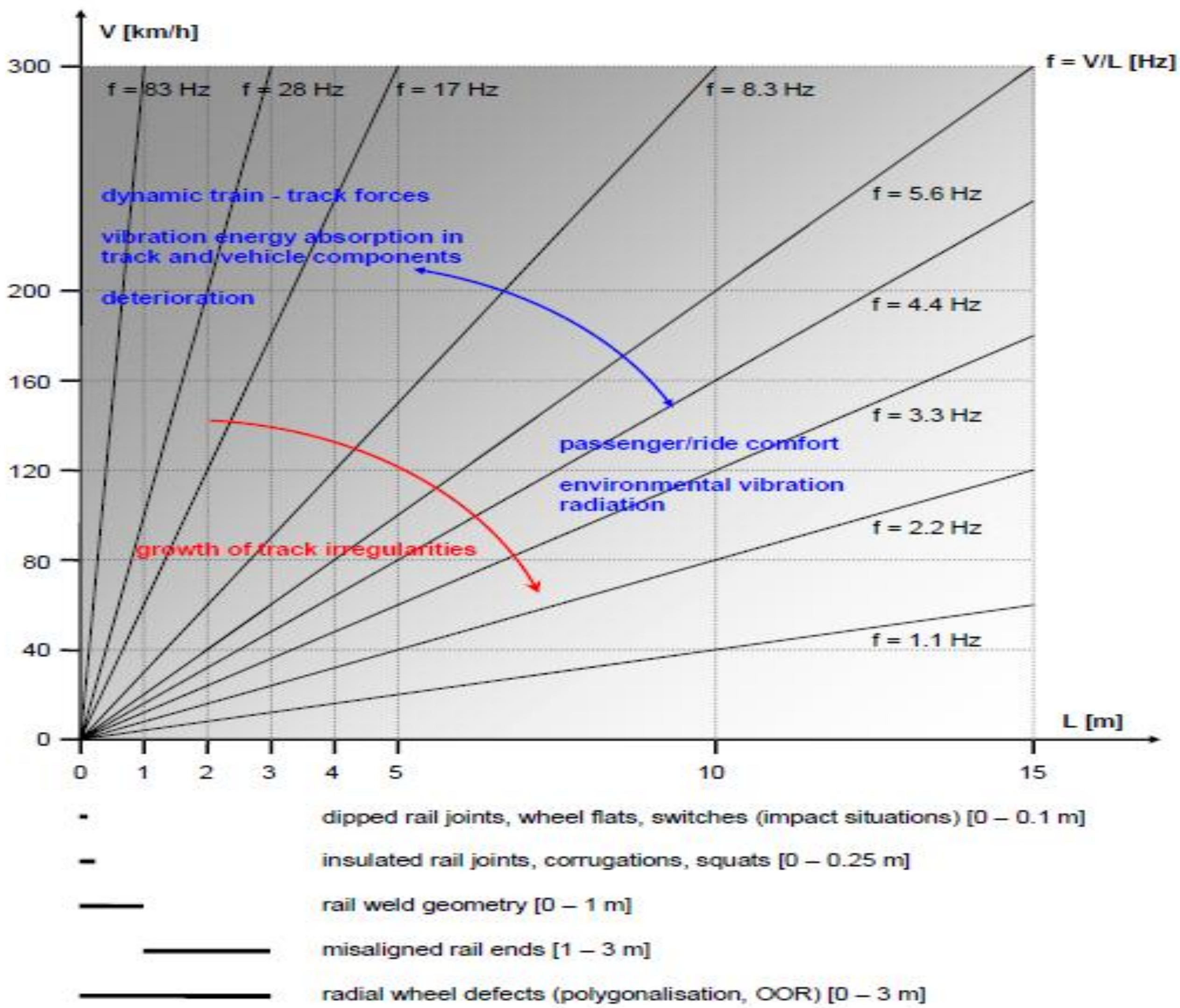

Fig. 2.1 Frequency diagram: coupling of wavelength *L* and speed *V* for typical wavelengths (short length-scales) in the train-track system. [33]

2.2 Overview of jointed rail

Different designs of rail joints are employed, for example supported and unsupported joints (depends on the position of the supporting sleepers) and inclined joints. Rail joints are generally weak spots of the track structure and have rather short service life as compared to the rail itself.

There is a high demand from the railway sector to increase the life span and reliability of these joints. The biggest problems by using rail joints gaps are the stress concentration on both ends of the rails caused by the imposed discontinuity.

The rail joint is assembled with two fishplates on both sides of the ends of the rail web and bolts to secure the connections, see figure 2.2 the gap between the two rail ends is varies among the different world countries.

Figure 2.2 Assembled rail joint

Several designs of rail joints are reported in the literature. The designs vary in terms of the parameters of the supporting systems and joint bars.

Two types of supporting systems of rail joints exist depending on the positioning of the sleepers with reference to the end post:

i) Suspended rail joints

ii) Supported rail joints

As shown in Fig. 2.3, the suspended rail joint has the sleepers positioned symmetric to the end post. For the suspended rail joints, there is no support underneath the end post. On the other hand, for the supported rail joint, the end post is placed directly on the sleepers

Figure 2.3 Suspended rail joints supported rail joints

The joint bar designs are characterized by various cross-section designs and the length of joint bar, namely 4-bolt joint bar and 6-bolt joint bar.

Joints are also made either square or inclined to the longitudinal axis of the rails. Fig.2.4 shows examples of these types of joints.

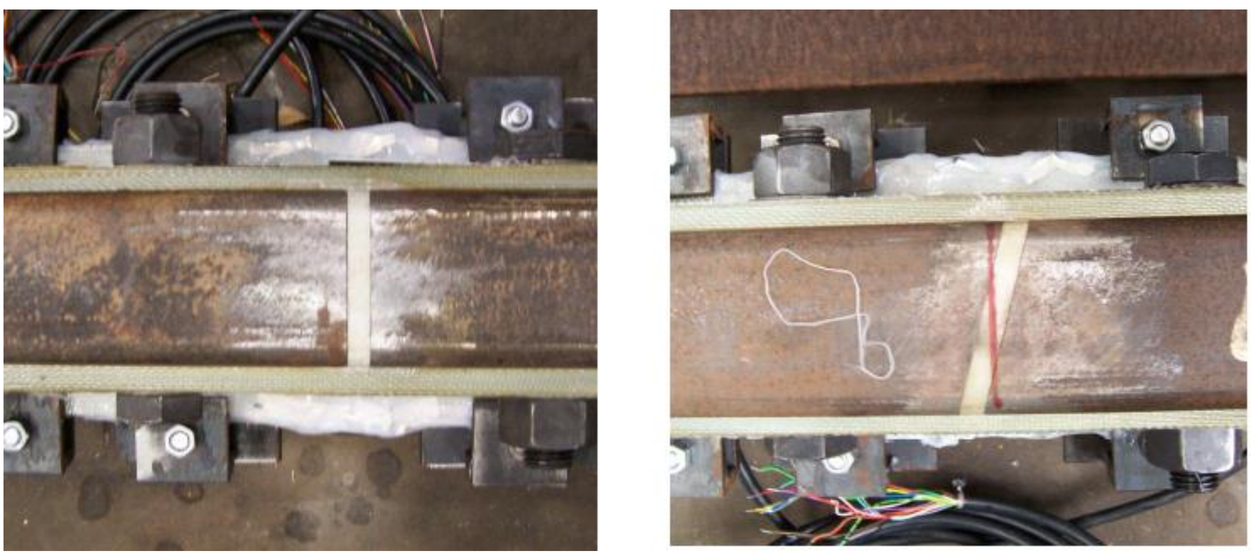

Square joints inclined joints

Figure 2.4 Types of Insulated Rail Joints

The gap size is also varied from 5mm to 20mm and is a key parameter for the rail joint design. The rail joints are laid on the "beddings" which contains several flexible layers. Two types of tracks exist, namely, 'conventional' ballasted track and 'non-ballasted' (for example slab-track) track. Most of the Ethiopian railway tracks are traditional ballasted and hence in this thesis only the ballasted track is chosen as the rail bedding.

2.3 Component of railway track

Rail track is a fundamental part of railway infrastructure and its components can be classified into two main categories: superstructure and substructure. The most obvious parts of the track as the rails, rail pads, sleepers, and fastening systems are referred to as the superstructure while the substructure is associated with a geotechnical system consisting of ballast, sub-ballast and subgrade (formation). Both superstructure and substructure are mutually important in ensuring the safety and comfort of passengers and quality of the ride. The typical shape and construction profiles of a track are illustrated in Figure 2.5.

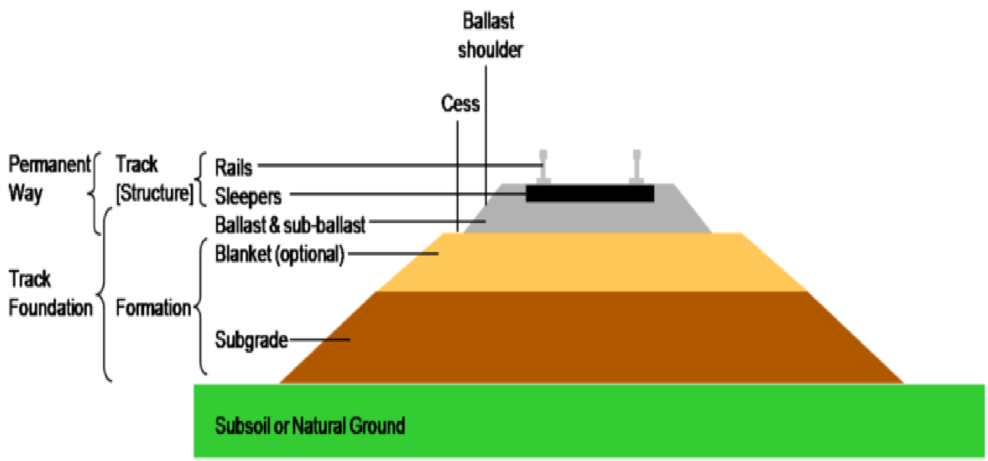

Figure 2.5 components of railway track

Rail

Rails are longitudinal steel members that are placed on spaced sleepers to guide the rolling stock. Their strength and stiffness must be sufficient to maintain a steady shape and smooth track configuration and resist various forces exerted by travelling rolling stock.

One of their primary functions is to accommodate and transfer the wheel/axle loads onto the supporting sleepers.

Lateral forces from the wheel sets, and longitudinal forces due to traction and braking of the train should also be transmitted to the sleepers and further down into the track bed. Rail defects and discontinuities, such as joints, can cause large impact loads, which have detrimental effects on the track components. The rails also act as electrical conductors for the signaling system. [26]

Rail pad and fastening system

The fastening system, or "fastenings," includes every component that connects the rail to the sleeper. Fastenings clamp the rail gauge within acceptable tolerances and then absorb forces from the rails and transfer them to the sleepers. Vibration and impact from various sources e.g. traffics, natural hazards, etc. are also dampened and decelerated by fastenings.

In a ballasted or ballast less railway track with concrete sleepers or beams, rail pads placed between the steel rails and the sleepers/beams to act as protector layers of sleepers from impacts, and provide electrical insulation of the rails. In the dynamic response of a track, the railpads play a vital role. [26] They influence the overall track stiffness. When the train loads the track, a soft rail pad allows a larger deflection of the rails, and the train axle load is distributed over wide area. Moreover, soft rail pads isolate the transmission of high-frequency vibrations down to the substructures. On contrary, a stiff rail pad gives a more direct transmission of the axle load, including the high-frequency load variations to the layers below the wheels. In ballast less tracks, the resilient property is mainly obtained from the rail pads.

Sleeper

The sleepers also called crossties are the transverse members of the railway superstructure. The main functions of sleepers are to distribute the wheel loads(vertical, lateral and longitudinal forces) transferred by the rails and fastening system to the supporting ballast, restrain rail movement by anchorage of the superstructure in the ballast which result in the provision of support to the rails so the sleepers preserve gauge, level, and alignment of the track. There are timber, steel and concrete sleepers. [26]

Ballast and sub ballast

The ballast and sub ballast layers support the track superstructure components (the rails and sleepers) against vertical and lateral forces from the trains. The ballast is a critical layer, which provided the primarily resilient property for the low frequencies (secondary suspension) and the rail pads for the high frequencies (primary suspension). Unfortunately, ballast is vulnerable to dynamic loads and it is not applicable after some train speed. Churning, flying, fouling and contamination of ballast are frequent problems in ballasted tracks, which undermines resilience property ultimately leading to exacerbated stresses in the system and possible component failures.[26]

2.4 Track Modeling

2.4.1 Beam Theories

2.4.1.1Euler-Bernoulli Beam (E-B beam)

In the E-B beam theory only bending of the rail is taken into account, and in case of vibrations, only the mass inertia in translation of the beam is included. To obtain an equation for the transverse vibration in a two-dimensional beam the following structure is studied. The beam is subjected to an external force and has a distributed mass m = ρA and flexural rigidity EI which can vary with position and time, which is shown in Figure 2.6.

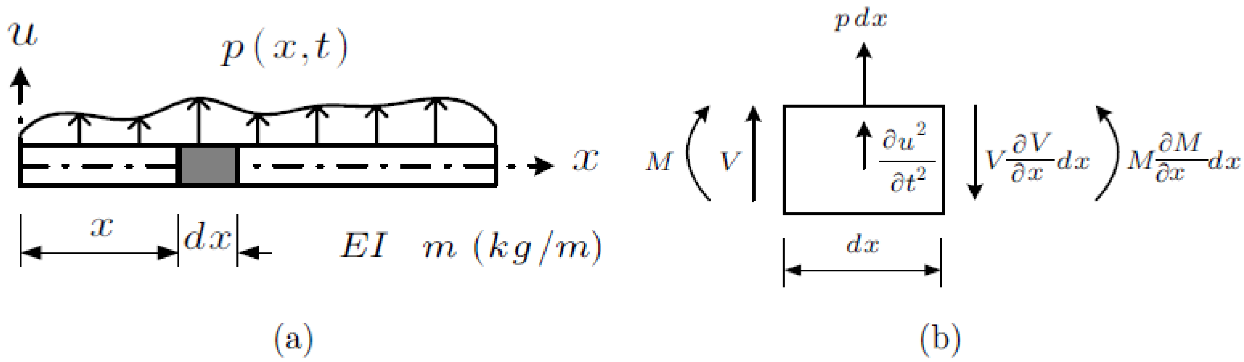

Figure 2.6: *(a) Beam and applied force, (b) force acting on an element*

The differential equation describing the beam deflection *w(x, t)* reads

$EI\,\frac{(\partial 4w(x,t)}{\partial x4} + \rho A\,\frac{(\partial 2w(x,t))}{\partial t2} = q(x,t)$……………………………………2.1

where,

EI = the bending stiffness of the beam

p = the density of the beam

A = cross-sectional area of the beam

q(x, t) = load on the beam

t = time

2.4.1.2 Rayleigh-Timoshenko Beam (R-T beam)

The R-T beam theory includes rotational inertia and shear deformation of the beam. In this case, two differential equations are needed to describe the vibrations. The deflection *w(x, t)* and the shear deformation ψ *(x, t)* are unknown functions. The differential equation for the deflection *w(x, t)* becomes

$$EI\,\frac{(\partial^4 \mathrm{w(x,t)})}{\partial x^4} + \rho\mathrm{A}\,\frac{(\partial 2\mathrm{w(x,t)})}{\partial \mathrm{t}2} + \rho\mathrm{I}\left[1+\frac{E}{(KG)}\right] * \left[\frac{\left(\partial^4 \mathrm{w(x,t)}\right)}{\partial \mathrm{x}^2\,\partial \mathrm{t}^2}\right] + \frac{\rho 2\mathrm{I}}{\mathrm{KG}} * \left(\frac{\left(\partial^4 \mathrm{w(x,t)}\right)}{\partial x^4}\right)$$
$$= q(x,t) \ldots\ldots\ldots\ldots\ldots\ldots .2.2$$

Where,

EI = the bending stiffness of the beam

G = shear modulus

k = shear factor

p = the density of the beam

A = cross-sectional area of the beam

q(x, t) = load on the beam

t = time

If the shear deformation of the beam is suppressed, i.e. if one gives *k* a very large number, then the two last terms on the left hand side tend to zero. Further, if the mass inertia in rotation of the beam cross section is eliminated (noting that $\rho I = \rho r^2 A = mr^2$, and let *r* tend to zero) then also the third term tends to zero and the E-B differential equation is obtained.

The Euler-Bernoulli theory assumes that the plan cross-sections, initially normal to the beam axis, remain plane, normal to the beam axis, and undistorted. All beam elements in ABAQUS that use linear or quadratic interpolation are based on this theory. The Timoshenko beam theory allows the elements to have transverse shear strain, so that the cross-sections don't have to remain normal to the beam axis. This is generally more useful for thicker beams.[27]

2.4.2. Winkler foundation Beam (rail) on continuous elastic foundation (BOEF)

In the most simple track model, a beam (that is an Euler beam model of the rail) rests on a continuous elastic foundation. The foundation is modeled by evenly distributed mutually independent (no interaction) linear spring stiffness. The distributed force supporting the beam then is directly proportional to the beam deflection and stress. The only track parameters needed for this model is the beam bending stiffness *EI* (Nm^2) and the foundation stiffness (the bed modulus) *k* (N/m^2, i.e. N/m per meter of rail). The rail deflection $w(x)$ (x is the length coordinate) is then obtained from the differential equation:

$$EI * \frac{\mathrm{d}d^4 4\mathrm{w(x)}}{\mathrm{kw(x)}} = q(x) \ldots\ldots\ldots\ldots\ldots\ldots\ldots\ldots\ldots\ldots..2.3$$

Where q(x) is the distributed load on the rail

This model may be acceptable only for static loading of a track on soft support; no dynamic effects can be analyzed using this model, as it contains no mass or inertia. However, the model can show the track uplifted in front and behind the wheel.

2.4.3 Pasternak Foundation Model

Pasternak model assumes shear interactions between the Winkler springs. This may be accomplished by connecting the ends of the springs to the beam consisting of incompressible vertical elements, which then only deforms by transverse shear. In *figure 2.7* the classical rail element on a Winkler foundation is extended with a shear element representing the interaction between the springs. The shear element is connected to the rail element. The distributed load on the rail is assumed to be zero. [19], [28] But, the model in which the rail is supported in a discrete manner, gives the better approximation than the Winkler's continuous support for ballasted track model. Such an approach also lends itself to the application of standard programs. These discrete and finite element method programs give great flexibility as regards load forms and support conditions. [29]

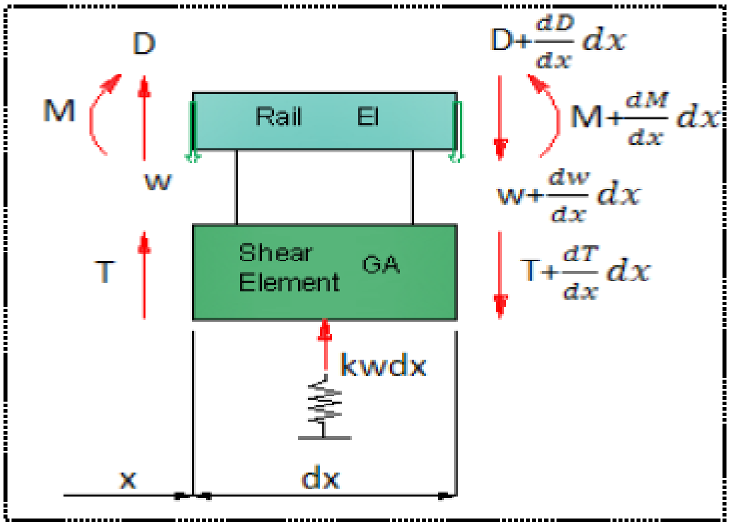

Figure 2.7 paster nak foundation for beam

2.4.4. Double Layer Beam Models

When the track structure is schematized as a double beam, in which the top beam represents the rail and the lower beam model the concrete beams. The upper beam, which represents the rail, has a distributed mass *m* and a bending stiffness *ErIr*. The RC beams are represented as a continuous beam with a mass m^2 and with some non-zero bending stiffness *EbIb* (zero for case of sleeper model in ballasted track). [29] The connection between the two beams consists of the rail pads with a stiffness *Kp* and a damping *Cp*. The formation layer can be modeled as elastic foundation with some damping and stiffness or it can be modeled as solid continuum media, which contributes some stiffness to the model.

2.4.5. Finite Element Modeling Using ABAQUS

The accuracy of any model depends on the strength of the software and its materials and element collection. ABAQUS has extensive library of finite and infinite modeling elements of almost all types of structural or mechanical modeling. Based on their section property and geometry, a model can contain one or a number of elements used to represent the physical problem. The accuracy of the model is also depends on the appropriate selection of the element and material definition.

Finite Element solver and modeling software, ABAQUS [27], provides multiple options to choose a dynamic, quasi-static or static analysis for almost any types of structures.

2.4.5.1. Linear Eigenvalue Analysis

Linear eigenvalue analysis is used to perform an eigenvalue extraction to calculate the natural frequencies and corresponding vibration modes of the track. The analysis can be performed using two different Eigen solver algorithms, Lanczos or Subspace. The Lanczos eigensolver is faster when a large number of Eigen modes are required while the subspace Eigen solver can be faster for smaller systems. [27]

2.4.5.2. Steady-state Dynamic Analysis

The Steady-state dynamic analysis in ABAQUS provides the steady-state amplitude and phase of the response of a system due to harmonic excitation at a given frequency. Usually such analysis is done as a frequency sweep by applying the loading at a series of different frequencies and recording the response. [27]

2.4.5.3. Implicit and Explicit Dynamic Analysis

The implicit dynamic analysis method is used to calculate the transient dynamic response of a structure. In an implicit dynamic analysis, the integration operator matrix must be inverted and a set of nonlinear equilibrium equations must be solved at each time increment. The general direct-integration method provided in Abaqus/Standard, called the *Hilber-Hughes-Taylor operator*, is an extension of the trapezoidal rule. The half-step residual is the equilibrium residual error halfway through a time increment, t+, $t+\Delta t/2$ and once the solution at $t + \Delta t$ has been obtained, the accuracy of the solution can be accessed and the time step adjusted appropriately.[27]

In an explicit dynamic analysis displacements and velocities are calculated in terms of quantities that are known at the beginning of an increment; therefore, the global mass and stiffness matrices need not be formed and inverted, which means that each increment is relatively inexpensive compared to the increments in an implicit integration scheme. The size of the time increment in an explicit dynamic analysis is limited, however, because the central-difference operator is only conditionally stable. The stability limit for the central-difference method (the largest time increment that can be taken without the method generating large, rapidly growing errors) is closely related to the time required for a stress wave to cross the smallest element dimension in the model. The time increment in an explicit dynamic analysis therefore, can be very short if the mesh contains small elements or if the stress wave speed in the material is very high. The explicit central-difference operator satisfies the dynamic equilibrium equations at the beginning of the increment, t; the accelerations calculated at time t are used to advance the velocity solution to time, $t+\Delta t/2$ and the displacement solution to time, $t+\Delta t$.

2.5 Wheel Rail Contact Dynamics

Contact is one of the common research topics because of its wide applications in the engineering field. The earliest theory of contact mechanics is due to the pioneering researcher Heinrich Hertz who published a classical paper on contact in 1882 in the German language. Subsequently several researchers improved the Hertz contact theory by relaxing the limitations and extending its application to more practical situations.

Hertzian contact theory

Hertz contact theory (HCT) is established based on some basic assumptions: elastic contact bodies, frictionless contact surfaces, continuous and non-conforming surfaces, small strains and small contact area relative to the potential area of contacting surfaces (35) .

According to Hertz theory, the normal pressure is distributed as an ellipsoid over the elliptic contact area with semi-axes a and b,

$$\frac{X^2}{a^2}+\frac{Y^2}{b^2}=1 \dots\dots\dots\dots\dots\dots\dots\dots\dots\dots\dots .2.4$$

$$A=\frac{a}{b} \dots\dots\dots\dots\dots\dots\dots\dots\dots\dots\dots\dots\dots\dots ..2.5$$

$$P_z\left({}^{x}/_{y}\right)=P_o*\sqrt{(1-(\frac{X}{a})^2-(\frac{Y}{b})^2} \dots\dots .2.6$$

$$P_o=\frac{3N}{2\pi ab} \dots\dots\dots\dots\dots\dots\dots\dots\dots\dots\dots 2.7$$

Where, Pz= wheel-rail contact stress,

N = normal force,

a and b= ellipse principal axes

Based on contact geometry, the relationship between force and deformation of the contact surface is not linear.

$$б=\frac{K}{\pi}\left(\frac{\pi\sum\frac{1}{r}}{2A^2E}\right)^{\frac{1}{3}}*\left(3\frac{(1-v)}{2G}\right)^{\frac{2}{3}}*(N)^{\frac{2}{3}} \dots\dots\dots\dots\dots\dots 2.8$$

$$б = K_n N^{\frac{2}{3}} \ldots\ldots\ldots\ldots\ldots\ldots\ldots .2.9$$

$$N = C_H * б^{\frac{3}{2}} \ldots\ldots\ldots\ldots\ldots\ldots\ldots .2.10$$

Linearizing about the static condition and assuming circular contact area with zero curvature of wheel profile, Hertzian spring contact can be simplified as;

$$N = K_H * б \ldots\ldots\ldots\ldots\ldots 2.11$$

$$K_H = \left(\frac{(3N)}{2}\right)^{\frac{1}{3}} * \left(\frac{E}{1-v^2}\right)^{\frac{2}{3}} * (R_w R_r)^{\frac{1}{6}} \ldots\ldots\ldots\ldots ..2.12$$

Where,б= penetration depth (over closure),

k_h= Hertzian spring,

E = equivalent elastic modulus of contact area,

v = poison's ratio,

R_w =wheel radius, R_r = rail radius

C_H= a constant depending on the contact surfaces radii and the material properties

The analytical solution of contact dimensions and pressure distributions between two smooth elastic bodies is obtained through the above process. This problem is strictly nonlinear because the displacement at any point of contact depends on the distribution of contact pressure throughout the whole contact zone. This leads to a significant complexity to solve the integral equations of contact pressure for each step in the dynamic contact condition. As a simplification, the 'Hertz contact spring' is developed.

2.6 Track dynamics of rail joints

In addition to the magnitude of the static axle load, reflecting the gravity loading of the train, the track performance is determined by the dynamic loading caused by the train-track interaction. At this time, numerous sources of track vibrations can be distinguished, which are a) wheel-rail contact irregularities which are rail irregularity or wheel flats, b) track structure irregularities which includes the sleeper distance, the discrete nature of the ballast, differential settlements, stiffness transitions in the subgrade or at bridges, tunnels and c) the velocity effect of the train.

[34]-states that the complex interaction of these track vibration sources are the origin for the mechanical processes that form the basis of track performance and track deterioration. These mechanical processes can be separated into two categories, according to [23] namely 1) short-term

mechanical processes and 2) long-term mechanical processes. The first category embraces the instantaneous, dynamic behavior of a railway track, as activated during the passage of one, or a few, train axles. The permanent track deformations generated during an individual train axle passage are usually very small, such that the track behavior may be viewed as reversible, and thus can be studied by means of (viscous) elastic models. The viscosity thereby is a measure for the energy dissipated during the reversible response. The second category embraces the mechanical processes characterized by a typically quasi-static time-dependency, such as, track deterioration due to subgrade particle migration into the ballast layer, or long-term sub structural settlements and long-term abrasion of rail profiles under a very large number of train axle passages. [23]

The sources of vibrations listed above may lead to track deterioration, such as rail head corrugation growth, damage to track components (rail pads, sleepers, ballast), track settlement, and soon. [24][25]

The dynamic effect of the discontinuity in the track

The vertical geometry of the track alignment is not constant along the length of the structure. Multiple discontinuities can be found in the track. These interruptions in the rail exist due to geometrical or material requirements.

Examples of track discontinuities are a common crossing in the geometrical design of a turnout ,an expansion joint to allow enlargement of the rail due to temperature changes ,an Rail Joint with bolts to connect two rail pieces and a welded joint to build a Continuous Welded Rail. The dynamic force amplification has been studied by several researchers. For instance, Jenkins [11] presents a model generated by the passing of a load over an rail joints. Figure 2.8 shows the time dependent behavior of Fdyn (dynamic forces) as the wheel of the train crosses over the joint.

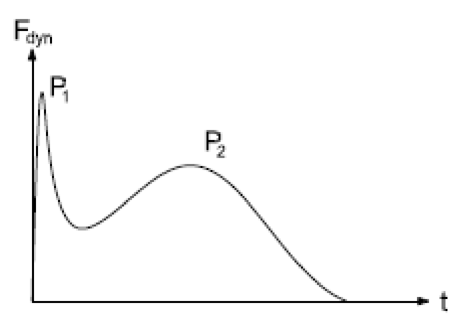

Figure 2.8: Dynamic force amplification in the case of rail joints

The model is dependent of the axle load, train velocity, mass and stiffness of the system, and the geometry of the irregularity (dip angle of the joint). The results of this study shows that, when the wheel of a vehicle crosses through rail joints, the vertical load is amplified.

2.6.1 Track Characteristics

Track design geometry (curves etc.) influences static and quasi-static forces, while track geometry quality is a main contributor to dynamic forces. Corrugation, often called rail roughness will generate high-frequency forces whereas rail imperfections such as joints or poor welds lead to impact forces. [18]

According to [30] track performance is regarded with respect to physical degradation factors which the author puts them in three. These are:-

2.6.1.1 Dynamic Effects

Traffic on most railway lines comprises many different forms of vehicle, varying from high speed passenger units to lower speed freight trains. Track is therefore subject to a wide range of bearing and bending stresses in the rails, pads, fasteners, sleepers, ballast and subgrade. These stresses come about not only because of the static mass of a vehicle, but also due to dynamic actions such as lateral centrifugal forces on curves, longitudinal acceleration and braking forces, vibrational forces induced from imperfections in the rail surface (corrugations, joints, welds, defects) and in the wheels (flats and shells), and from the dynamic response of the track components to these actions.

The consequences of the frequently large forces generated by these actions are many and varied. Fatigue cracking in rails, plastic flow or shelling out of the rail head, uneven wear of the rail head, cracking or splitting of sleepers, loosening of fasteners, grinding and redistribution of ballast, and variations in track alignments and gauge are the major deleterious effects. Such effects result in poor riding quality, reduced train speed, increased fuel consumption, potential derailment, increased maintenance, delays and reduced level of service.

2.6.1.2 Train Speeds

Increasing the speed of trains has many effects on rail and track performance and degradation, from literatures [30] it has been deduced that higher speeds cause greater track deflections, can significantly influence the deterioration of track geometry, and is one of the key factors affecting the wheel/rail impact loads; these loads produce very high bending stresses in rails and in sleepers. However, studies concluded that speed may not influence dynamic vertical wheel loads. Clearly there are many sources of dynamic forces and the effect of train speed upon these forces has not been established definitively. It is certain, yet, that higher train speeds result in greater operating costs for rolling stock and increased track maintenance activity.

2.6.1.3 Axle Loads

Axle loads affect rail head wear, fatigue of the rail steel, and plastic flow and shelling in the running surface between wheel and rail head. Greater axle loads lead to increased wheel wear and higher bending stresses in rails and sleepers, as well as higher bearing stresses in ballast. [28]

2.6.2 Dynamic Properties of Rail pads and Fasteners

The rail pads play a significant role when the point of discussion is track dynamics. The overall track stiffness is influenced by rail pads. A soft rail pad permits a larger deflection of the rails when the track is loaded by the train. Hence the axle load from the train is distributed over more sleepers. The stiffness of the fastening is normally much less than that of the rail pad. Therefore, when a wheel set loads the track, only the rail pad stiffness is important. For an unloaded rail, however, the fastening will induce a certain preload (static load) on the rail pad. Therefore, when investing track dynamics the role of the fastenings is normally neglected.

The spring-damper system is the most commonly used physical model of a rail pad. The spring can be assumed to be linear, and the damping is assumed to be proportional to the deformation rate of the rail pad. According to the comparison between track models and measurements it's important to include the rail pads to get an accurate track model. From measurements, the type of rail pad also influence the dynamics of the track that soft rail pads would result in lower sleeper acceleration and higher railhead acceleration than the stiff rail pads. [1][5]

2.6.3. Dynamic Properties of Sleepers

Considering the sleeper in modeling as either a rigid mass for frequencies below 100 Hz or as a flexible beam is a matter of interest to obtain what results from model. For frequencies up to 300 or 400 Hz, the Euler-Bernoulli beam theory may suffice. At higher frequencies, the Rayleigh-Timoshenko beam theory should be used for an accurate description of the sleeper vibration.

Along the rail, the stiffness changes because it is supported by sleepers separated by a distance around 50 cm. The stiffness is higher when the wheel passes at the level of a concrete sleeper. These vibrations induced by the sleeper distance have a frequency f given by the equation 2.9 where V is the speed of the train and D is the distance between two sleepers. [4][5]

$$f=v/\lambda \quad \ldots\ldots\ldots\ldots\ldots\ldots\ldots \quad (2.9)$$

2.6.4. Dynamic Properties of Ballast, Subballast and Subgrade

The complex interaction between ballast particles makes their behavior not fully recognized as it is a complex medium because of its granular properties. Generally the ballast distribute the loads from the sleepers to the soil through the sub ballast. Most often, a layer of sub ballast will be included in the design which prevents the penetration of the ballast particles into the soil or vice versa. The ballast is constituted by stone particles. A granular media can have behavior both like solids and liquids: on one hand, the ballast supports sleepers; on the other hand, the liquefaction of ballast is a dangerous problem which can cause derailment. Without any train loadings, internal forces in the ballast are low. During train passages, the friction between particles increases and the ballast is compressed by the train loading. [4]

CHAPTER THREE

MODELLING AND MODELLING PARAMATERS

Strategy-1: Simplifications of Geometry Modeling

The complexity of the rail joints and the wheel geometry demands simplifications to reduce the computational cost. For the rail joint, as attention is focused on the dynamics of the rail joint and the rail track at and around the rail joint, the finite element model was simplified to just one part model by ignoring the interaction between the contact surfaces of the rail, the joint bars, the bolts, and the nuts.

It is fairly complex to simulate the behavior of rail joint. The effect of the rail joints are affected by the characteristics of the rolling stock and that of the rail joints itself. The dynamics of the rolling stock is idealized as pure rolling of the wheel.

Since this research focus is on effect of the rail joints, the geometry of wheel cross-section is also simplified. Since the flange contact is out of our scope, the wheel flange is firstly removed and the wheel cross-section is also simplified in which the wheel with a shape of circle is investigated in this thesis. An actual train wheel has "conic" shape as sketched in figure 3.1 However, for making of the wheel simple and less complex, the wheel was modeled as circle.

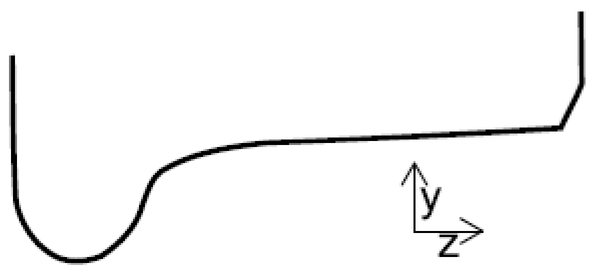

Figure 3.1 Surface profile of real train wheel

3.1 Boundary Conditions

Under pure rolling, the wheel rotates at an angular velocity ω that corresponds to the linear velocity *v*. The wheel motion is restrained in the lateral direction; in other words, DOFs 5 and 6 (Fig. 3.2) are arrested.

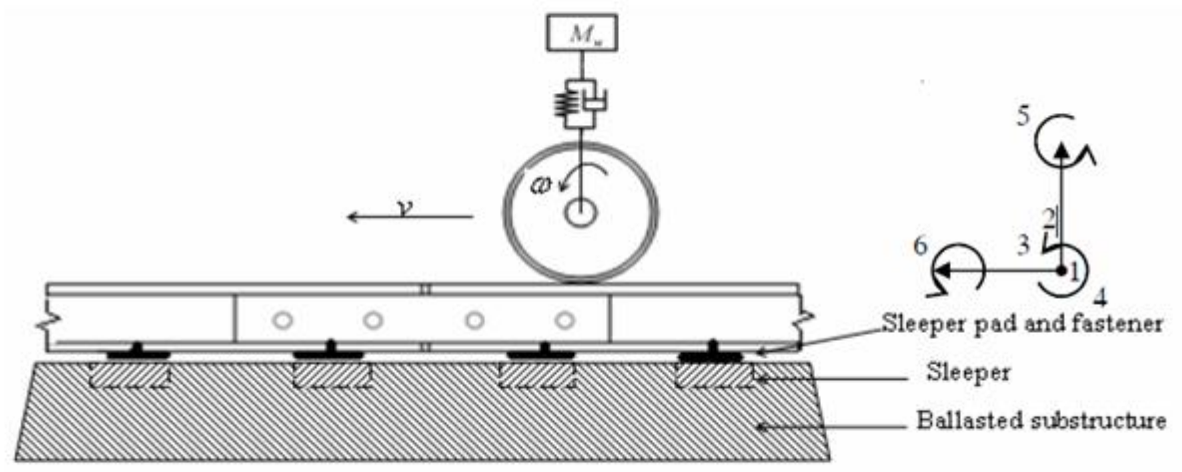

Figure 3.2 Boundary conditions of wheel and rail joints

Strategy-2: Simplifications of Material Modeling

The mechanical property of modeling material is listed in the table below. There are different types of tracks. Thus, I have used AVE Zaragoza track for the modeling, since the AVE Zaragoza track type is the track having 1.435mm track guage, the rail cant of 1/40, the rail of CN60 and the sleeper pitch of 600mm which is almost similar with track that has been found in Ethiopia.

Table 3.1 Mechanical property of modeling material [34]

Mechanical Properties	
Vehicle characteristics	
Car bodies mass	58,400 kg
Wagon mass moment of inertia about Y axis	617,282 kgm2
Bogie mass	3,600Kg
Bogie moment of inertia	1,801 kgm2
Primary suspension stiffness	6,500KN/m
Primary suspension damping	10KNs/m
Secondary suspension stiffness	2,555KN/m

Secondary suspension damping	30KNs/m
Wheel Load	112.5KN
Model rail length(m)	12m each rail
Ballast thickness(m)	0.3m
Sleeper spacing(m)	0.5m
Steel Density	7,800 kg/m3
Steel Young's modulus	210Gpa
Steel Poison ratio	0.3
Rail pad Stiffness (MN/m)	100
Rail Pad Damping(MNs/m)	0.015
Sleeper Density	2,500kg/m3
Sleeper Young modulus	35Gpa
Sleeper Poison ratio	0.22
Ballast Density	1,600
Ballast Young modulus	210Mpa
Ballast Poison ratio	0.3
Ballast stress distribution angle	0.8
Ballast internal friction	45^0
Ballast Dilation angle	15^0

3.2Druckers- Prager model

Sleepers, rails, and rail pads were introduced into the model as elastic linear materials. This simplification cannot be adopted for granular materials (foundation, embankment, blanket, ballast, and sub ballast). Although these materials have an elastic response under very low levels of stress, they exhibit a plastic behavior under higher stresses [31]. For this reason, elastic plastic behavior was assumed.

The most appropriate model to represent this phenomenon is the Drucker-Prager model [32] which is based on the hydrostatic stress. It shows that an elastic plastic response of the granular material is suitable for the modeling. This model of behaviour may be introduced in ABAQUS by implementing the angles of internal friction (Φ_i) and dilatancy (Φ_d) of each material.

Friction Angle

The peak friction angle of ballast is conveniently calculated from the triaxial test results of peak principal stress ratio, by rearranging the Mohr-Coulomb failure criterion, as given in the following relationship:

$$\left(\frac{\sigma_1}{\sigma_3}\right)_p = (1 + \sin(\emptyset_p) \ldots \ldots \ldots \ldots \ldots \ldots \ldots .3.1$$

ϕ_p is the peak friction angle, σ_1 is major principal stress and σ_3 is minor principal stress..

From the above equation we can easily derive

$$\emptyset_p = \arcsin\left(\frac{q_{peak}}{(2\sigma_3 + q_{peak})}\right) \ldots \ldots \ldots \ldots \ldots \ldots \ldots \ldots \ldots 3.2$$

Where q_{peak} is maximum deviator stress. Thus above equation relates the peak frictional angle with the peak deviator stress.

Dilation Angle

The dilation angle (ψ) is calculated from the slope of the expansive portion of volumetric strain versus axial strain increase. The slope is calculated by a linear fit to the data from the greatest volumetric contraction to the end of the test. The dilation angle calculation expression is

$$\psi = \frac{d\varepsilon_y}{d\varepsilon_a} \ldots \ldots \ldots \ldots \ldots \ldots \ldots \ldots \ldots \ldots \ldots \ldots \ldots \ldots 3.3$$

3.3 Strategy-3: Simplifications of modeling

The rail joint is supported on the ballasted substructure with sleepers and sleeper pads placed at the bottom of the rail.

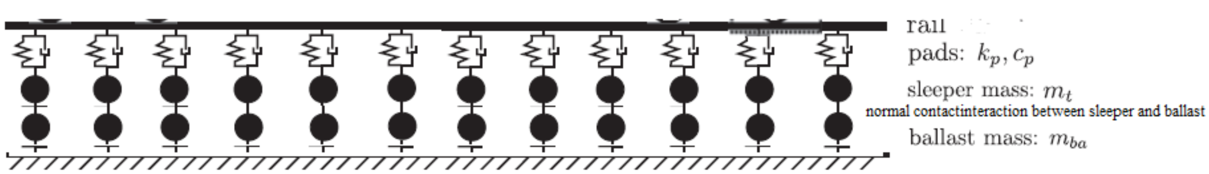

Fig. 3.3. The rail support system

In this modeling, the height of 17cm of the rail having length 24m and jointed rail at the middle of the length is used for modeling. Under the bottom the rail the sleeper having spacing of 50cm is placed under all the entire of the rail length.

Further, at each location of the sleeper the rail pads having a stiffness of 100MN/m and damping of 15000Ns/m is incorporated on the top of the sleeper. Finally, the ballast of having a thickness of 30 cm is placed under the sleeper.

In similar way the vehicle having 46cm of wheel radius and vehicle characteristics having the primary and secondary suspension stiffness and dumping is considered during the modeling and for further clarification see figure 3.4. As it is clearly seen from the figure below that rail length having of 24m and sleepers having 50cm spacing is considered during the modeling. Further, regarding to the vehicle characteristics, the vehicle wheel having 46 cm radius and having of primary and secondary suspension stiffness and damping has been also considered.

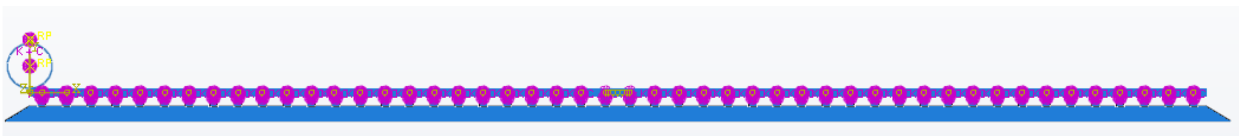

Figure 3.4 Modeling

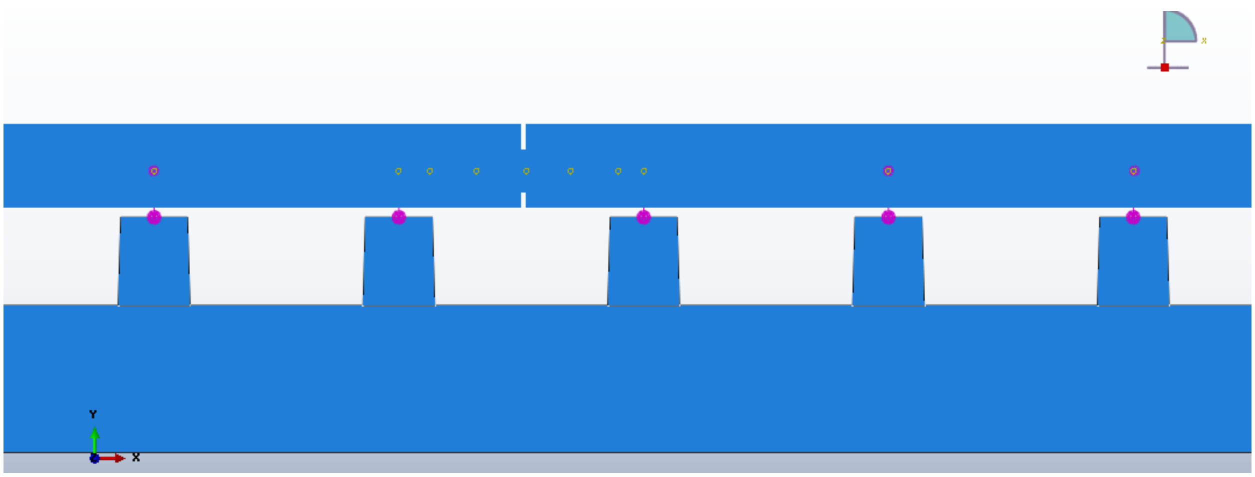

Figure 3.5 jointed rail

Strategy-4: Boundary conditions of the wheel

Proportion of wagon mass is transferred to the wheel through the suspension system as shown in Fig. 3.6. The proportional mass is obtained by dividing the gross wagon mass by the number of wheels.

The suspension system is simplified into a single layer spring/damping model using a formula of:

$$\frac{1}{K}=\frac{1}{K_1}+\frac{1}{K_2}\ldots\ldots\ldots\ldots\ldots\ldots\ldots\ldots\ldots\ldots\ldots\ldots\ldots\ldots\ldots..3.4$$

Where K is the combined and simplified stiffness

K_1 Primary suspension stiffness

K_2 Secondary suspension stiffness

$$\frac{1}{K}=\frac{1}{6500}+\frac{1}{2555}$$

K=1,834.07KN/m

$$\frac{1}{D}=\frac{1}{D_1}+\frac{1}{D_2}\ldots\ldots\ldots\ldots.3.5$$

Where

D is the Combined and simplified damping

D_1Primary suspension damping

D_2Secondary suspension damping

$$\frac{1}{D}=\frac{1}{10}+\frac{1}{30}$$

D=7.5KNs/m

Table 3.2 primary and secondary suspension stiffness and damping (AVE Zaragoza track type)

Primary suspension stiffness	6500KN/m
Primary suspension damping	10KNs/m
Secondary suspension stiffness	2555KN/m
Secondary suspension damping	30KNs/m

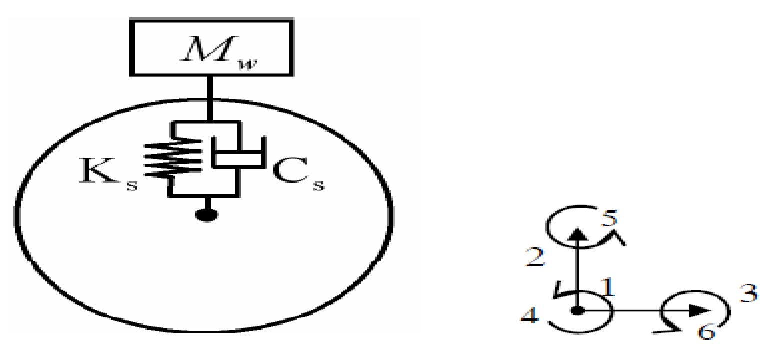

Figure 3.6 The wheel Loading system

In the static wheel/rail contact model, the wheel DOF 2 is free and DOFs 1 and 3 are arrested. In the dynamic analysis, the lateral motion of the wheel is restrained to ensure the contact stability before impact. The wheel DOFs 2 and 3 are set free. For the pure rolling condition, the wheel body is assigned an initial condition of rotating speed around its center axis and a longitudinal velocity v which is defined as the product of rotating speed and the radius.

Strategy-5: Wheel/Rail Contact Modeling

Definition of rail/wheel contact interaction in ABAQUS is very sensitive to convergence, accuracy of result, and computational time. Thus careful definition of the rail/wheel contact is the key to the impact dynamic analysis.

In the modeling, the master/slave contact surface method is employed for the dynamic analyses. The surfaces of the wheel are defined as the master, and the railhead is defined as the slave. The contact surface pair is allowed to undergo finite sliding. The interface friction is described with the Coulomb friction law by defining a friction coefficient. In the normal direction, the pressure-over closure relationship is set to HARD meaning that surfaces transmit no contact pressure unless the nodes of the slave surface contact the master surface.

CHAPTER FOUR

RESULTS AND DISCUSSION

4.1. Introduction

The results of the dynamic effect of the jointed rail on the railway track components obtained from the finite element modeling and analysis ABAQUS are presented in this chapter. The dynamic analysis including natural frequency extraction, modal dynamic and dynamic explicit analysis is utilized to study the dynamic effect of jointed rail on the rail way track components. Further, the lateral and vertical modes are extracted to examine the dynamic jointed rail response. Moreover, in order to further analyze the dynamic effect of the jointed rail on the rail way track components, the vehicle speed effect, the sleeper's position effect whether placed as suspended or supported sleeper, the rail pads stiffness effect and wheel loads effect on the railway track response are also studied using dynamic explicit analysis.

4.2 Results of Dynamic Analysis

4.2.1 Natural frequency Analysis

The response of the natural frequency analysis is highly associated with extracted modes of vibration. The extracted modes of vibration should be extracted to provide a good representation of the dynamic response of the track structure. So that, extracting of sufficient number of eigen values modes of vibration is important especially in representing enough modal of effective mass participation in each degree of freedom and in each direction of the extracted modes.

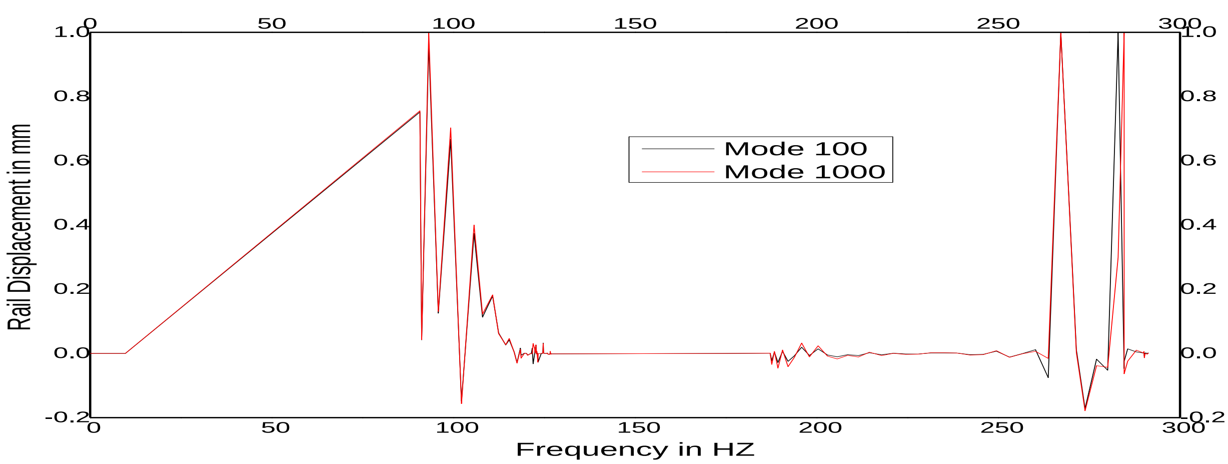

Figure 4.1 the effect of Eigen frequency modes of vibration extracted for rail vertical deflection for 100 and 100 modes of extraction

As shown in the above figure that the number of modes to be extracted whether it is to be 100 mode of vibration or 1000, it doesn't have a significant difference in the vibration of the track and seems serviceable that the dynamic responses of the railway track structure associated with the lower modes of vibration. The rail deflection and frequency intensity of the rail are propagates in similar patterns for almost 100 and 1000 modes extracted.

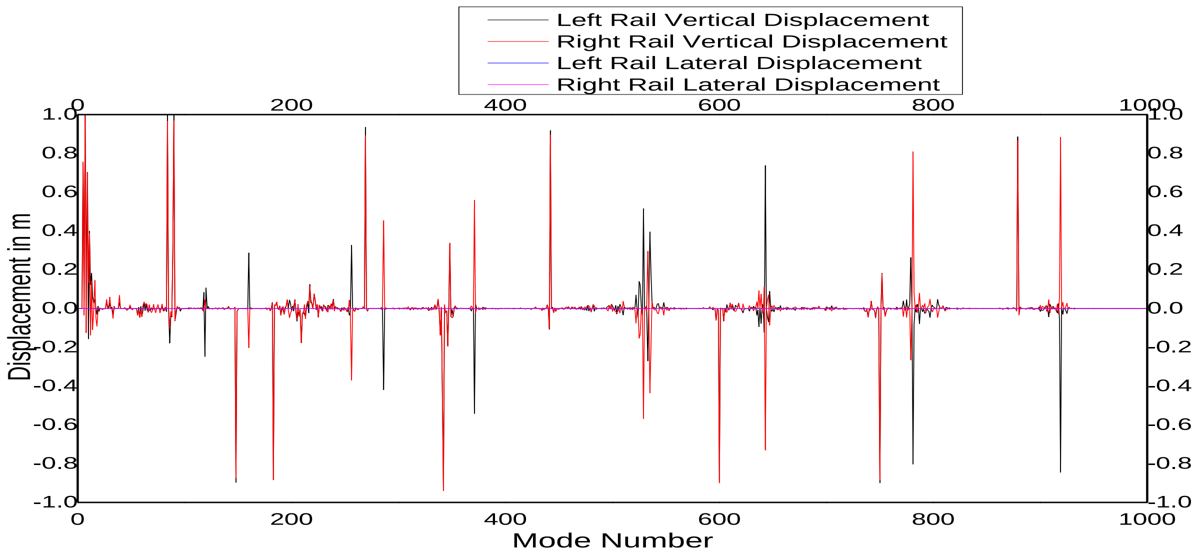

Figure 4.2 rail vertical displacement for the first 100 modes of vibration

As we can see from the above figure 4.2 that the rail vibrates and dominates in the vertical upward direction for the first 200 modes of vibration and then the dynamic vibration in the vertical down and upward directions are almost equal. This indicates that, the lower mode of vibration gives a good representation in analyzing and studying the dynamic effect of the jointed rail on the railway track structure.

<u>Vibration modes</u>

According to the given excitation input, the model of the rail way track vibrates in different forms of shapes when the modeled railway track is analyzed in the ABAQUS software. Thus, the vibration modes of the rail way track are related to resonant frequencies; these frequencies are characteristic of the system.

According to [26], the vibration of the railway track structure is divided into three groups of mode (Table 4-1).

Range of Frequency (Hz)	
Low	0-40
Mid	40-400
High	400-1500

Table 4-1: Frequency ranges for railway track vibration

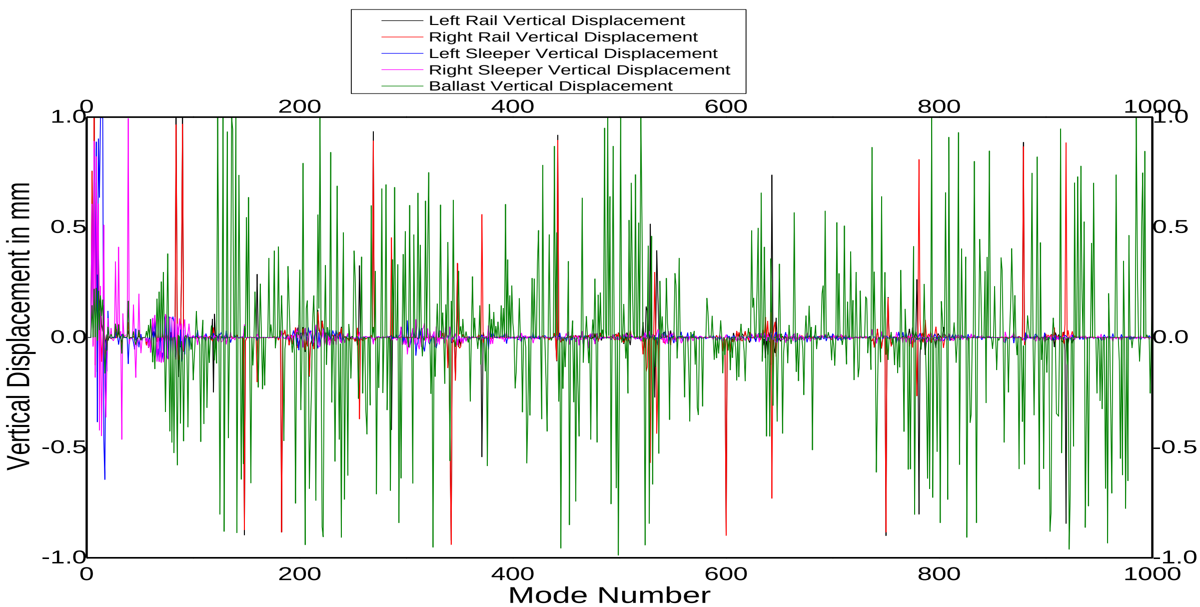

Figure 4.3 rail, sleeper and ballast vertical displacement for the first 1000 modes of vibration

As we can see from the above figure that the rail and sleeper vibrates and dominates in the vertical upward direction for the first 100 modes of vibration and then the ballast vibration takes the domination in the vertical upward and down ward direction for the modes of vibration goes from 100 to 1000. This indicates that, the dynamic vertical vibration response of the rail and sleeper can be represented and explained easily in the lower modes of vibration. However, conversely the ballast vertical vibration can be easily represented and explained in the higher modes of vibration. Furthermore, the results show that the right rail and sleeper vibrates and dominates highly in the vertical direction than the left rail and sleeper for the first 100 modes of vibration.

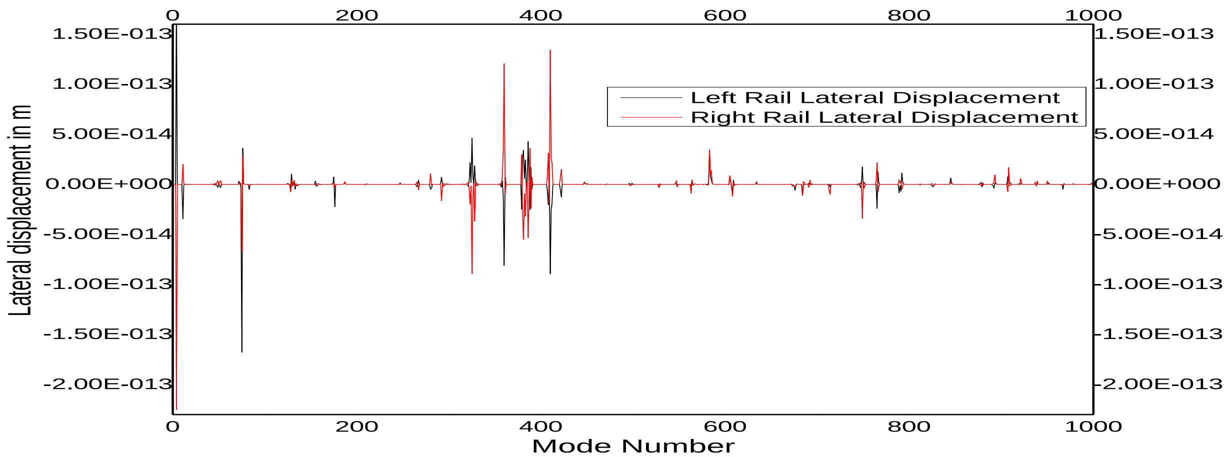

Figure 4.4 Rail lateral displacements for the first 1000 modes of vibration

As we can see from the above figure that the lateral vibration of the left rail vibrates and dominates in the vertical upward direction and conversely the lateral vibration of the right rail vibrates and dominates in the downward direction at the first modes of vibration. However, for other modes of vibration, the lateral vibration of the left and right rail looks quite similar except at the mode of vibration from 300 to 410 in which the lateral vibration of the right rail dominates the lateral vibration of the left rail.

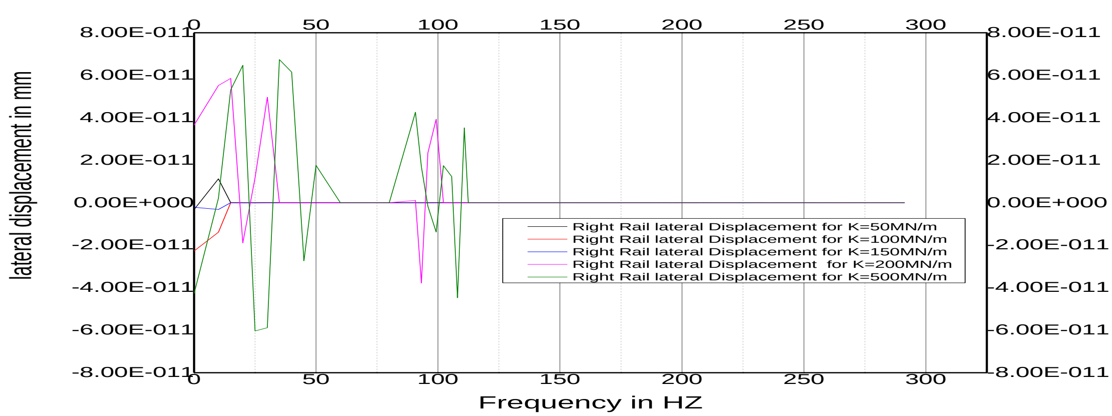

Figure 4.5 Right rail lateral displacements

As we can see from the figure 4.5 and 4.6 that the lateral displacement of the rail is higher and dominant between the frequency range from 0HZ to 50HZ.

The pattern and shape as well as the lateral vibration modes of the left and right rails look quite similar for the first 50HZ frequency range and also at around100HZ. However, their magnitudes are differing.

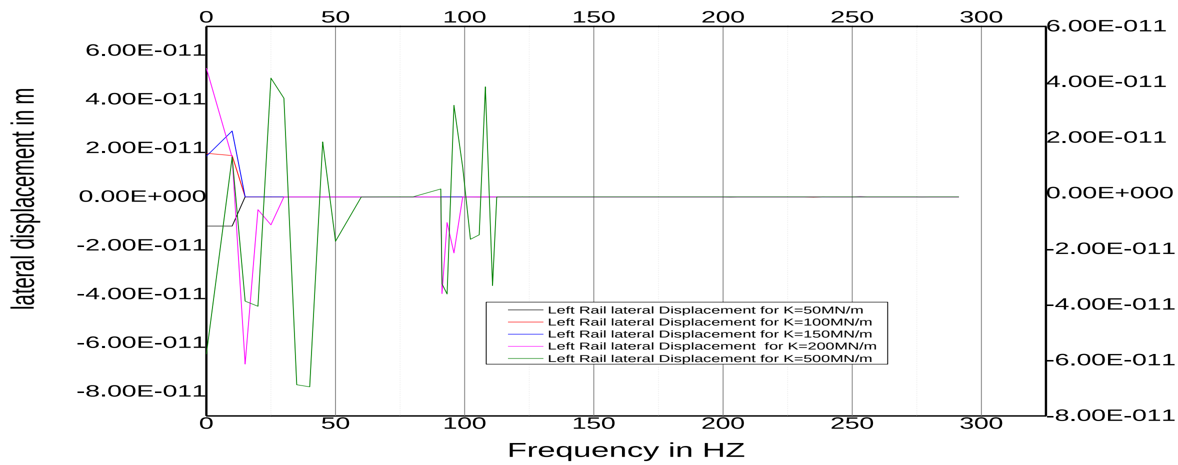

Figure 4.6 Left rail lateral displacement

As a general, in this study, the vibration of the rail track corresponds to almost the mid frequency range (40Hz to 400Hz). Further, as we can see from the figure 4.7 that with this mid frequency range, the whole element of the track such as rail, sleeper and ballast vibrates bends as a whole. However, even though all elements of the rail tracks structure vibrate and bend as whole, its magnitudes vary.

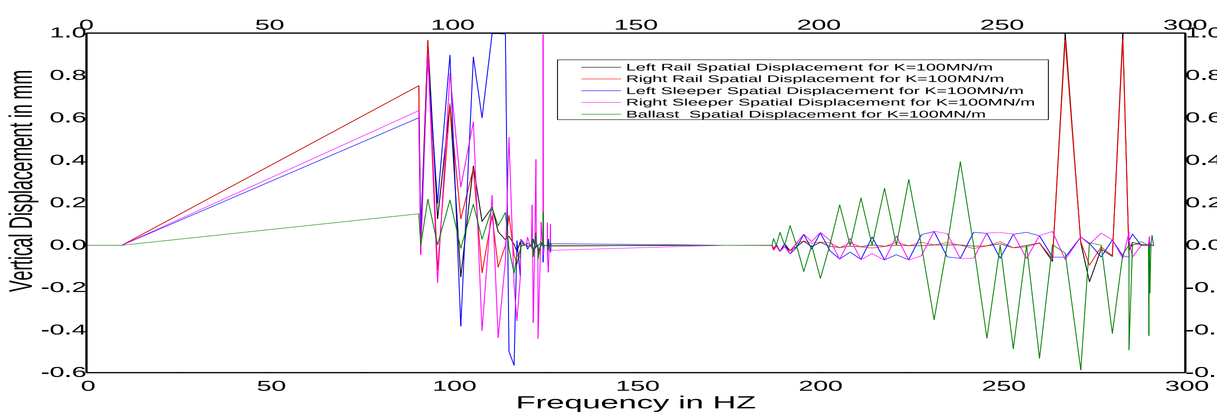

Figure 4.7 Rails, sleeper and ballast vertical displacement

For example, the vertical vibration of the rail, sleeper and ballast is almost zero and constant at the initial frequency and conversely, the lateral displacement of the rail is higher at the initial frequency [see figure 4.5 and 4.6]. Thus, the analysis result indicates that at the initial frequency range, the lateral vibration of the railway track element is greater than the vertical vibration. In addition to this, the vertical vibration of the rail, sleeper and ballast is almost zero and constant at the initial frequency. This is because of the connection constraints condition between track components. The vertical connection constraints condition between the track components at the initial frequency range is stronger than the lateral connection. Due to this, the vertical vibration of the rail, sleeper and ballast is zero and constant at the initial frequency range. However, when the vertical vibration of the rail, sleeper and ballast reach certain frequency range, the vertical vibration modes of the railway track components takes the domination from the lateral direction and become straight and getting to increase for the frequency range from 20HZ to 90HZ.

After that, the increment of the vibration in vertical direction continues for all railway track components even though their results is differ. Comparing their results, the rails vertical vibration and movements is higher than sleeper and ballast for the frequency ranges from 90HZ to 130HZ.

Moreover, for describing it in detail, the vertical vibration of the rail, sleeper and ballast is higher at the frequency 90HZ and smaller at the frequency 130HZ. Even if it is higher at 90HZ and smaller at 130HZ, the vertical vibration of the rail, sleeper and ballast is not continuously increased or decreased rather moved in zigzag patterns between the frequency ranges from 90HZ to 130HZ.

It is known that the vertical vibration modes of the rail, sleeper and ballast are almost zero for the static motion since there is no movement at the static stage and higher for the dynamic stage. For example, as we can see from figure 4.7 that, for the frequency ranges from 130HZ to 174HZ, the vertical vibration of the rail, sleeper and ballast is getting small and small for the reason that the movement of the track appears to be static and no dynamic vertical vibration at this frequency range. Thus, the frequency range from 130HZ to 174HZ cannot affect the vertical vibration of the railway track so that the railway track appears to be static during the modeling.

Nevertheless, for the frequency range from 174HZ to 300HZ, the vertical vibration of the railway track start to be changed from the static to dynamic and as result its magnitude starts to increase and reaches maximum. As we can see from the figure 4.7 that, the dynamic effect of the vertical vibration of the rail and sleeper is higher in magnitude than the ballast for frequency range from 0HZ to 174HZ. This happens due to the dynamic impact of the jointed rail is higher at the top parts of the railway track and smaller at the bottom parts of the railway tracks. However, as the magnitude of frequency is getting higher and higher, the higher stress developed on the top parts of the railway track will be distributed to the bottom parts of the railway track. As a result, the vertical vibration at the bottom parts of the railway track will become higher. Hence, increasing the frequency range from 174HZ to 300HZ, it creates higher vertical vibration on the bottom parts of the railway track. Thus, for the above mentioned reasons, the dynamic vibration of the bottom parts of the railway track or ballast is higher at the frequency range from 174Hz to 300HZ. Moreover, In order to further analyze the dynamic effect of the jointed rail on the rail way track components, the rail pads stiffness effect on the railway track response are also studied for each railway track components (rail, sleeper and ballast).

Effect of the rail pads stiffness

The stiffness or softness of the rail pads has an important effect in absorbing the vibration undulations of the track. In this thesis, the rail, sleeper and ballast vibrational amplitude within the first 100 requested modes of vibration are studied in the ABAQUS software.

Further, in order to minimize the modes vibration of the rail, sleeper and ballast, rail pads having a stiffness range from 50MN/m to 500MN/m are introduced and analyzed. The results show that the vibration mode of the rail is larger for the rail pads stiffness of 500MN/m and smaller for the rail pads stiffness of 50MN/m. In this regards, it is known that as the rail pads stiffness is getting to be stiffer and stiffer, the rail vibration modes will be minimized. However, in this study, as the rail pads stiffness increase from 50MN/m to 500MN/m, the vibration modes of the rail becomes greater and greater for the frequency range from 90HZ to 130HZ and the reverse for other frequency range. Thus, from this we can conclude that the rail pads stiffness cannot minimize the vibration modes of the rail for all frequency range.

1. Rail Vertical Vibration

As the frequency goes from 0HZ to 90HZ and from 130HZ to 185 HZ, the vertical vibration of the rail has almost similar shape for all rail pads stiffness even though having different stiffness. However, for the frequency range from 90 Hz to 130 Hz and 189HZ to 215 HZ, the rail vertical vibration is become vary as the rail pad stiffness is differ.

Further, as we can see from figure 4.8 that, as the stiffness of the rail pads increases from 50MN/m to 500MN/m, the vertical vibration of the rail placed at the left side of the jointed rail will also increase. However, this is not true for all frequency range from 0HZ to 300HZ. Because of the vertical vibration of the rail will also decreases at the someplace as the stiffness of the rail pads increase from 50MN/m to 500MN/m. Thus, from this diagram, it is clearly seen that increasing of the rail pads stiffness by itself will not totally reduce the dynamic vertical vibration of the rail.

Comparing the rails placed at the right and left side of the jointed rail, both of them have similar rail vertical vibrational shape except at same points in which the direction of the undulation pattern are moved in opposite direction.

Further, as we can see from the figure 4.8 that at the frequency range from 90HZ to130Hz the rail vertical vibration is higher in magnitude for all rail pads stiffness and at the frequency range from 182HZ to 267Hz, the rail vertical vibration is higher in magnitude for the rail pads having stiffness of 100MN/m and 50MN/m even though their magnitude is different.

Thus, the rail pads stiffness of 50MN/m and 100MN/m is not preferable for the frequency range from 182HZ to 267HZ since their vertical vibration is maximum for the said frequency range. However, the rail pads stiffness of 150MN/m, 200MN/m and 500MN/m is more preferable for the frequency range from 182HZ to 267HZ since the vertical vibration of the rail is almost small and similar.

Further, it is known that the vertical vibration of rail is not constant for all the frequency range and also can be zero if it is static. For example, in this study for the frequency range from 134HZ to 185HZ, the vertical vibration of rail is almost zero even though there is somewhat small vertical vibration. Thus, at this frequency range the dynamic effect of the rail vertical vibration is not severe that means it is almost static.

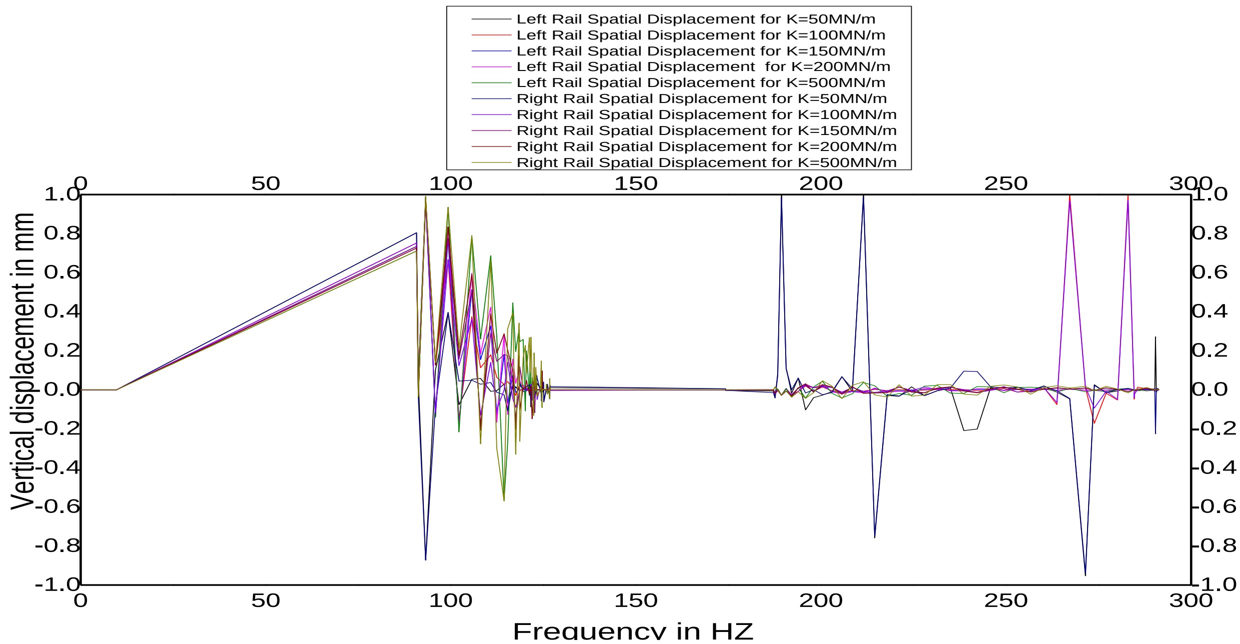

Figure 4.8 Rail to the left and right side of Jointed rail spatial Displacement

2. Vertical Vibration of sleeper

The vertical vibration of the sleeper placed to the right and left side of the jointed rail have externally similar shape except at the same point in which the direction and the location of the vertical vibration is differ. Similarly, as it is clearly described in the above vertical vibration of the rail, the vertical vibration of the sleeper is also higher in magnitude and also highly varied in zigzag forms for small frequency range from 90HZ to 134Hz. However, for the remaining frequency range from 182 HZ to 300HZ, the vertical vibration of sleeper is almost small. For example, for the frequency range from 134HZ to 182HZ, the dynamic vertical vibration of the rail and sleeper is almost zero owing to the vertical vibration of the rail and sleeper is static at this frequency ranges.

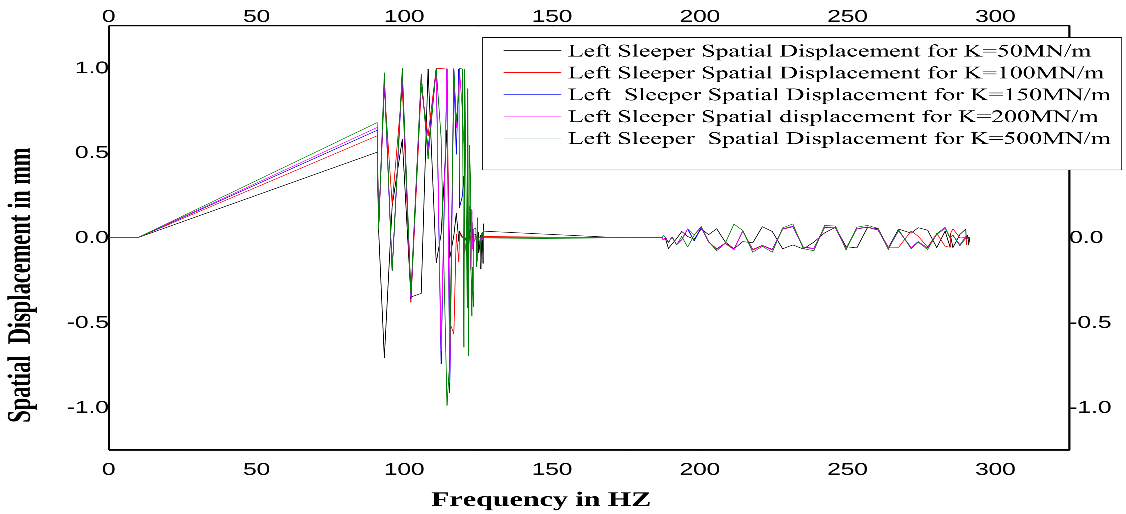

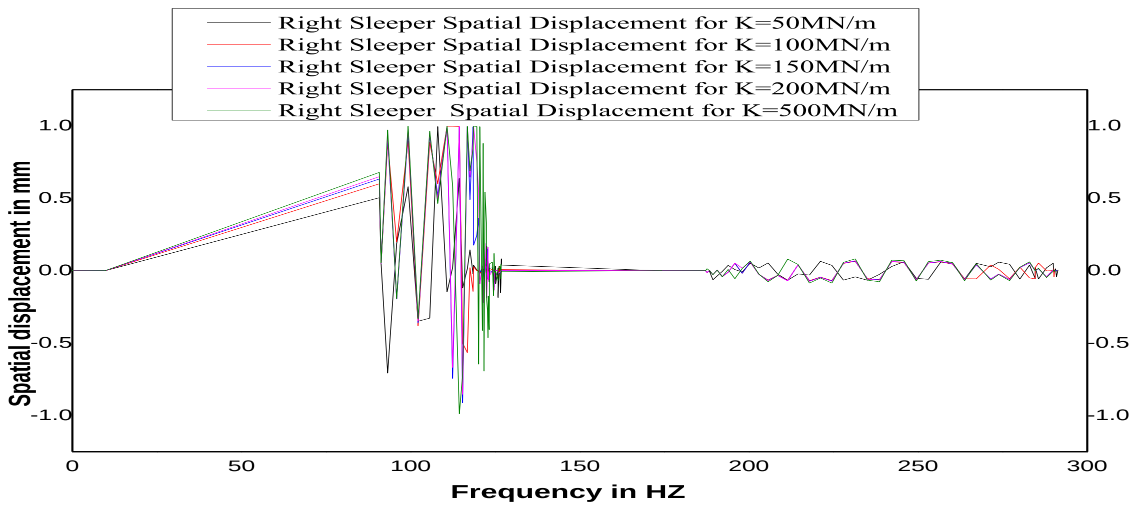

Figure 4.9 Frequency of the Left and Right sleeper

3. Ballast Vertical Vibration

As we can see from the above discussion that, the vertical vibration of the rail and sleeper is high and maximum for the frequency range from 0HZ to 134 HZ. However, in case the ballast the result is the reverse. That means, the vertical vibration of the ballast is small comparing to the vertical vibration of the sleeper and rail for the above said frequency range. Furthermore, the vertical vibration of the ballast can also be zero for static movement. For example, the vertical vibration of ballast is zero for the frequency range from 134Hz to 182HZ owing to its movement is static. As the frequency range is going to be higher, the dynamic vertical vibration is to be higher on the bottom parts of the railway track. Thus, for the frequency range from 182HZ to 300Hz, the vertical vibration of the bottom parts of the railway track or ballast is higher. Generally, comparing the result of the dynamic vertical vibration of the ballast with rail and sleeper, we can conclude that the magnitude of the vertical vibration of the sleeper and rail is greater than the ballast for the frequency range from 0 to 174 Hz and vice versa for the frequency range from 174 Hz to 300 Hz.

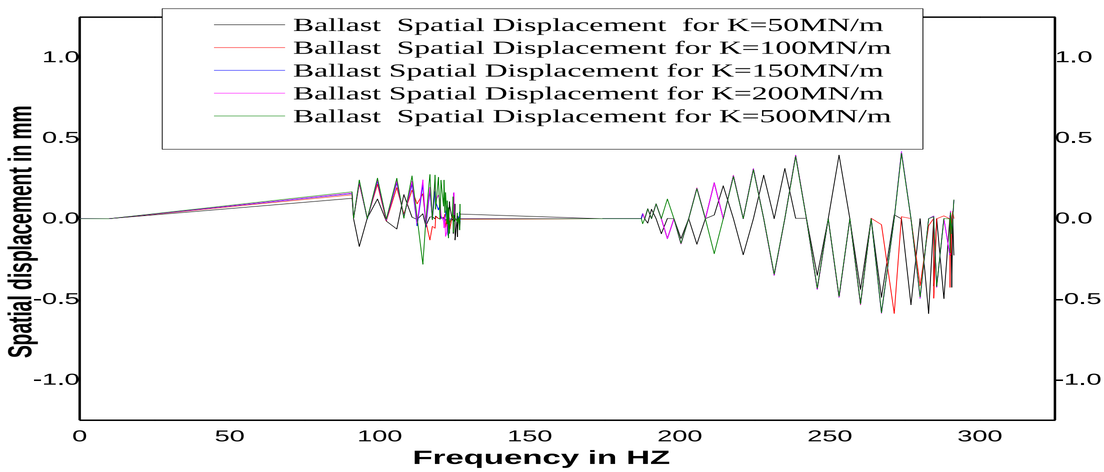

Figure 4.10 Frequency of the Ballast

Generally we can conclude from the above section that;

1. The vertical vibration of the rail and sleeper is almost straight line for the frequency range from 0HZ to 90HZ. However, for the frequency range from 90HZ to 130 HZ, the dynamic vertical vibration of the rail and sleeper is highly varying in zigzag forms.
2. The vertical vibration of the rail, sleeper and ballast is almost zero for the frequency range from 130 HZ to 182HZ owing to the dynamic vertical vibration of the track is almost zero and it is simply static loading.
3. The vertical vibration of the ballast is higher than the rail and sleeper for the frequency range from 174 Hz to 300Hz. Thus, special attention shall to be given for the ballast for this frequency range.
4. The Rail Pad stiffness of 50MN/m and 100MN/m is not preferable for the frequency range of 182HZ to 300HZ owing to the dynamic vertical vibration of the rail for this rail pad stiffness is higher at this frequency range.

5. The vertical vibration of the rail and sleeper is maximum at the frequency range of 90Hz to 130Hz and the vertical vibration of the ballast is maximum at the frequency range of 174Hz to 300Hz. Thus, special attention shall to be given for the rail and sleeper in the frequency range of 90Hz to 130Hz and for the ballast in the frequency range of 174Hz to 300Hz either by increasing of the rail, sleeper and ballast material strength or by any means.

4.2.2 The Dynamic Explicit Analysis

The dynamic explicit procedure performs a large number of small time increments efficiently. An explicit central-difference time integration rule is used; each increment is relatively inexpensive (compared to the direct-integration dynamic analysis procedure available in Abaqus/Standard) because there is no solution for a set of simultaneous equations.

4.2.2.1 Acceleration

In this study the acceleration of the rail, sleeper and ballast for the dynamic effect of jointed rail on the railway track is studied. Thus, the study indicates that the acceleration of the rail, sleeper and ballast is maximum around the middle of the jointed rail. This is happened for the reason that the dynamic effect of the jointed rail is high.

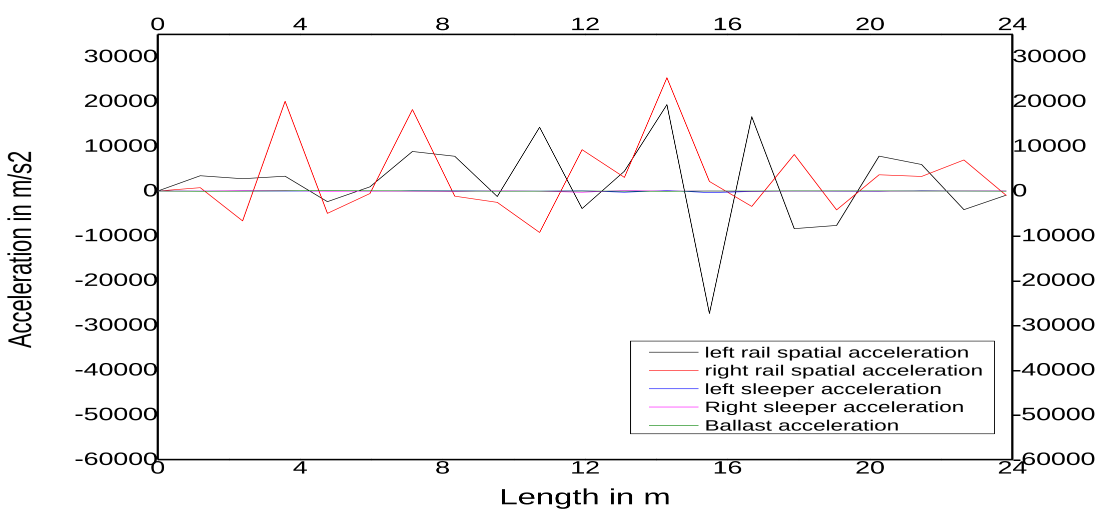

Figure 4.11 Acceleration of rail, sleeper and ballast as the vehicle moves from left to the right direction

As we can see from the above diagram that the acceleration of the rail is greater than the sleeper and ballast. Further, comparing the left rail acceleration with right rail acceleration, both rails have more or less smooth acceleration at the initial and ending points. However, at the middle of the length, the acceleration of the rails looks zigzags shape and also its magnitude is maximum than at initial and ending point of the length.

Moreover, the acceleration of the rail is higher than the sleeper and ballast as the vehicle move from left to the right side direction and vice versa. Further, comparing the acceleration of the left and right rail, we understand that the acceleration of the left rail is higher and more dominantly than the right rail as the vehicle moves from the left to the right direction and the acceleration of the right rail is higher and more dominantly than the left rail as the vehicle moving from right to the left direction.

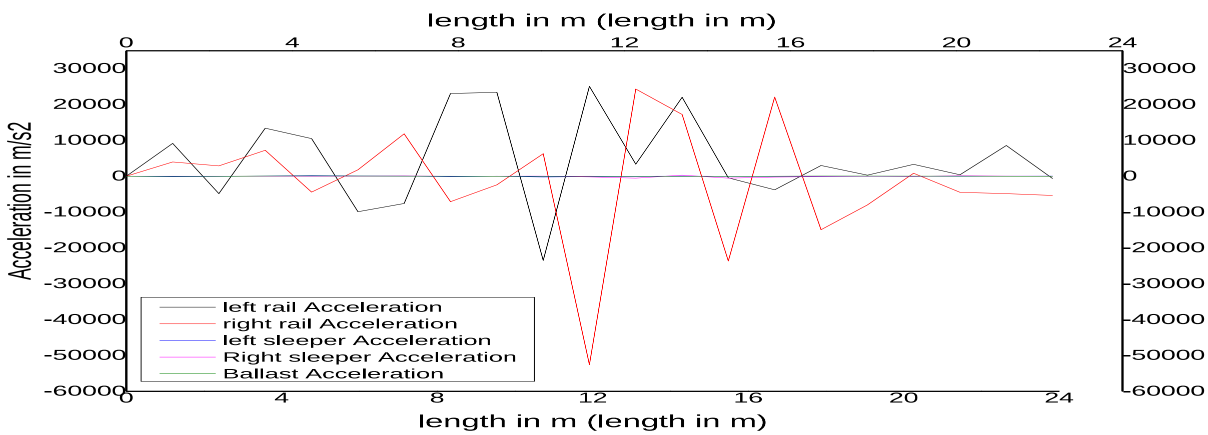

Figure 4.12 Acceleration of rail, sleeper and ballast as the vehicle moving from right to the left direction

As a general we can conclude that when the vehicle moves from left to the right direction, the acceleration of rail, sleeper and ballast is higher relatively near to the left side of the jointed rail owing to that of the dynamic effect of the left side of the jointed rail is higher. In similar way, the acceleration of the rail, sleeper and ballast is higher relatively at the right side of the jointed rail when the vehicle is moving from the right direction to the left direction.

2. Spatial displacement

In this thesis, in addition to the vertical and lateral vibration of the railway track, the spatial displacement of the rail, sleeper and ballast are also analyzed using the dynamic explicit modeling in the Abaqus software. [27] Further, in order to further examine the dynamic effect of the jointed rail on the railway track, the following scenario was examined in the ABAQUS software for modeling the dynamic effect of the jointed rail on the railway track components:

1. The effect Vehicle speed
2. The effect of rail pad stiffness
3. The position of the sleeper (whether the rail joint is placed on the sleeper and between the sleeper)
4. The effect of wheel diameter
5. The number of wheel in the modeling parts

As wheel starts rolling over the rail, the dynamic effect of the rail, sleeper and ballast is almost small at the initial for the reason of the wheel loads is nearly static at the initial stage. However, as wheel continues its rolling over the rail, its dynamic effect is becoming higher and higher. Further, as the wheel movement reach at the jointed rail, the dynamic effect of the jointed rail creates high impact load on the rail, sleeper and ballast. As a result, the spatial displacement of the rail, sleeper and ballast becomes maximum at this jointed rail. However, when the rolling of the wheel passes the jointed rail, the dynamic effect of the jointed rail on the railway track components becomes zero at the ending point.

Generally, we can conclude that, the spatial displacement of the rail, sleeper and ballast becomes zero at the initial and ending points and; maximum at the jointed rail or at the middle of the rail. See figure 4.13.

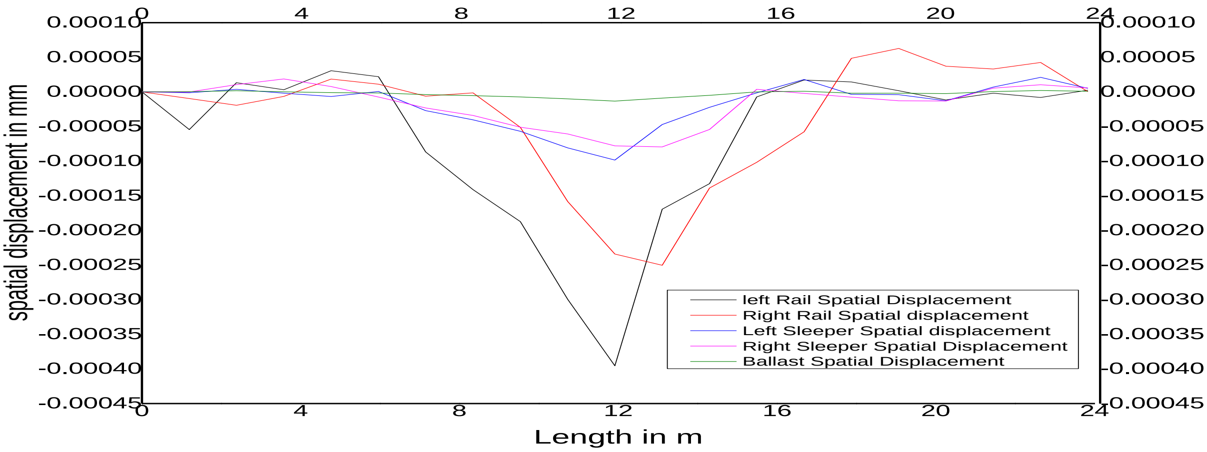

Figure 4.13 Spatial displacement of rail, sleeper and ballast

The above results of the dynamic effect of the jointed rail on the railway track components are presented in detail in section below. Moreover, in order to further analyze the dynamic effect of the jointed rail on the railway track components, the effect of the vehicle speed, rail pads stiffness, position of sleepers, wheel load and diameters are also presented.

1. **Effect of Vehicle speed**

   - **Rail Spatial displacement**

As we can see from figure 4.14 that, as the vehicle speed of the train increases, the spatial displacement of the rail is also vary in zigzag form for all entire length of the rail. However, as it is clearly seen from the figure 4.14 that, at the middle of the rail length or at the placement of the jointed rail, the spatial displacement of the rail placed at the left side of the jointed rail is maximum. Further, as the vehicle speed of the train increases from 60Km/hr to 200Km/hr, the spatial displacement of the rail is also increases.

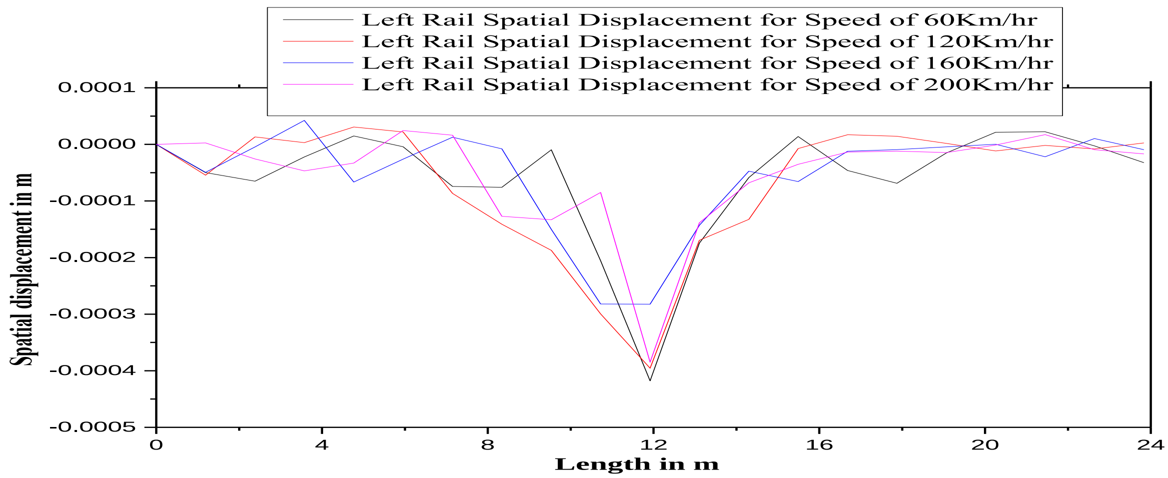

Figure 4.14 Spatial displacement of the rail placed to the left side of rail joint

Similarly, the spatial displacement of the rail placed at the right side of the jointed rail is also vary in zigzag forms, as the vehicle speed of the train increases from 60Km/hr to 200Km/hr. As it is clearly seen from the figure 4.14 and 4.15 that, even though both rails placed at the right and left side of the jointed rail has variant profile along the entire length of the rail, the maximum spatial displacement of the rail is observed at the middle of the length which is at 12m or at the placement of the jointed rail. From this result, we can conclude that, the spatial displacement of the rail is higher at the jointed rail and smaller for the rail placed away from the jointed rail.

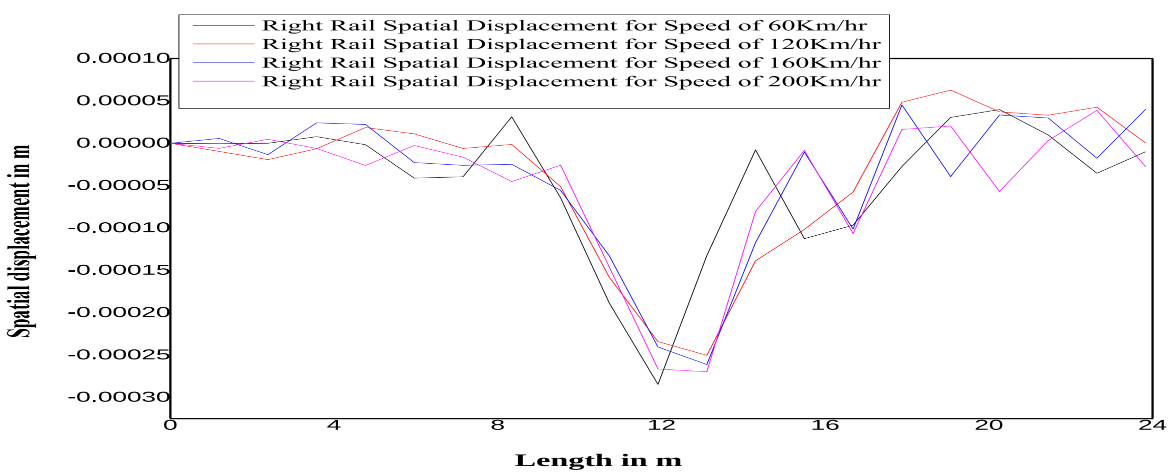

Figure 4.15 Spatial displacement of the rail placed to the right side of rail joint

- **Sleeper**

As it is seen from the figure 4.16 and 4.17 that, as the train starts rolling on the rail, the spatial displacement of the sleeper placed at the left and right side of jointed rail travel in the upward direction for the vehicle speed of 160 Km/hr. However, after some movement of the trains on the rail, the spatial displacement of the sleeper goes in the down ward direction for all vehicle speed of the trains and also the shape of the spatial displacement of the sleeper looks vary in zigzag forms for all the entire length of the rail. Thus, even though the spatial displacement of the sleeper is vary in zigzag forms as the vehicle speed of the train is vary, the highest and maximum spatial displacement of the sleeper is observed at the middle of the rail or at the placement of jointed rail. In light with this, the spatial displacement of the sleeper increases at this jointed rail as the vehicle speed of the train increases from 60Km/hr to 200Km/hr.

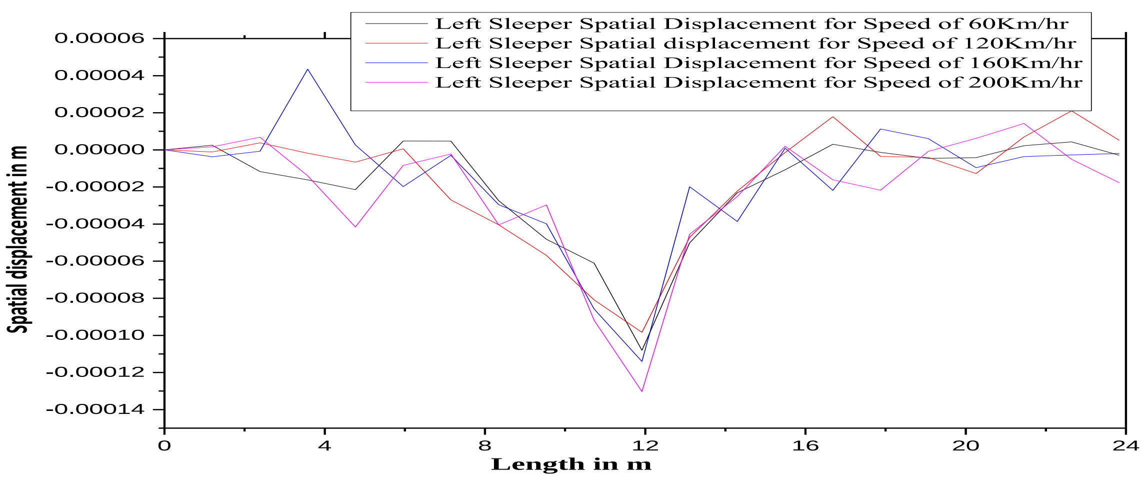

Figure 4.16 Left side sleeper spatial displacement

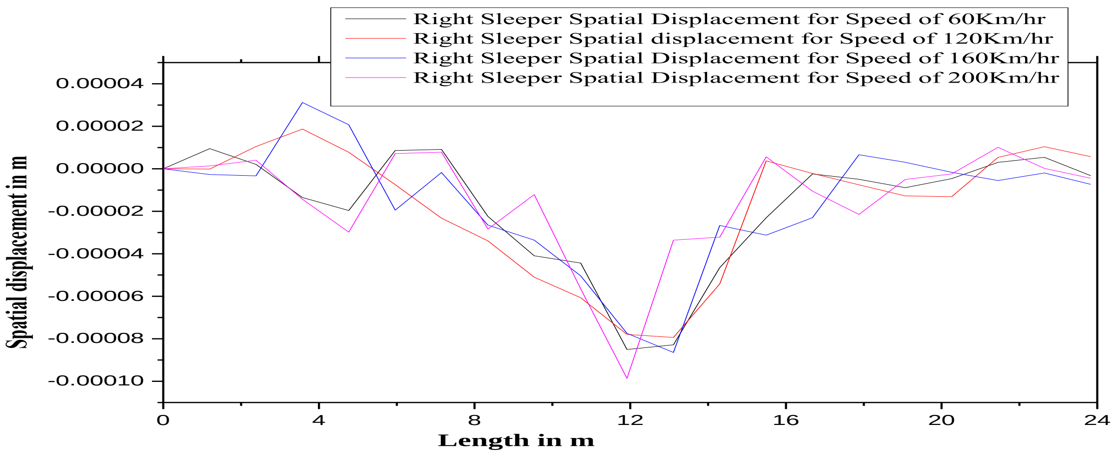

Figure 4.17 Right side sleeper spatial displacement

- **Ballast**

Similarly, as the wheel starts rolling on the rail, the spatial displacement of the ballast is also move in the upward direction for the frequency of 160Km/hr. However, after the movement of the train on the rail continues, the spatial displacement of the ballast is getting to be vary as the vehicle speed is vary except at and around the jointed rail or at 12m, in which at this location that as the vehicle speed increases from 60Km/hr to 200Km/hr, the spatial displacement of the ballast is also increases.

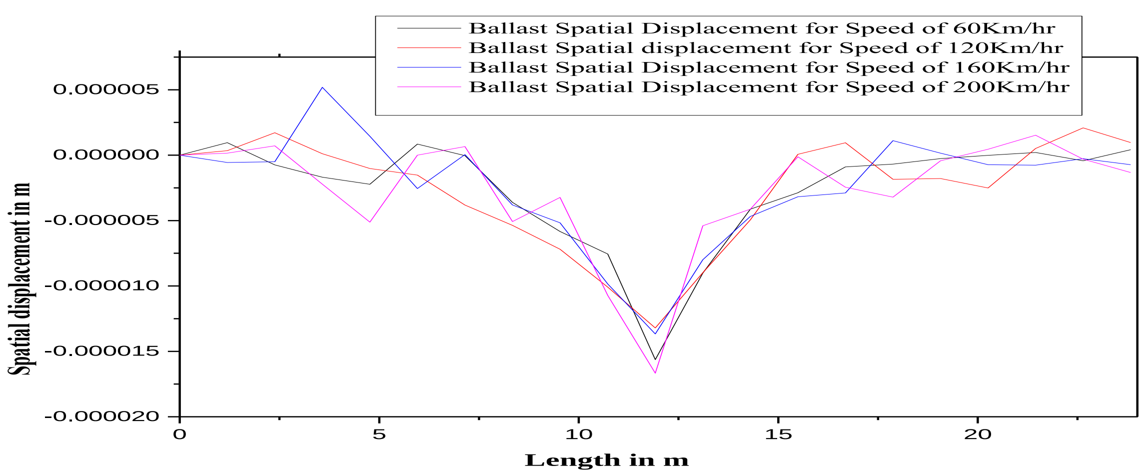

Figure 4.18 Ballast spatial Displacement

Spatial displacement of the rail, sleeper and ballast

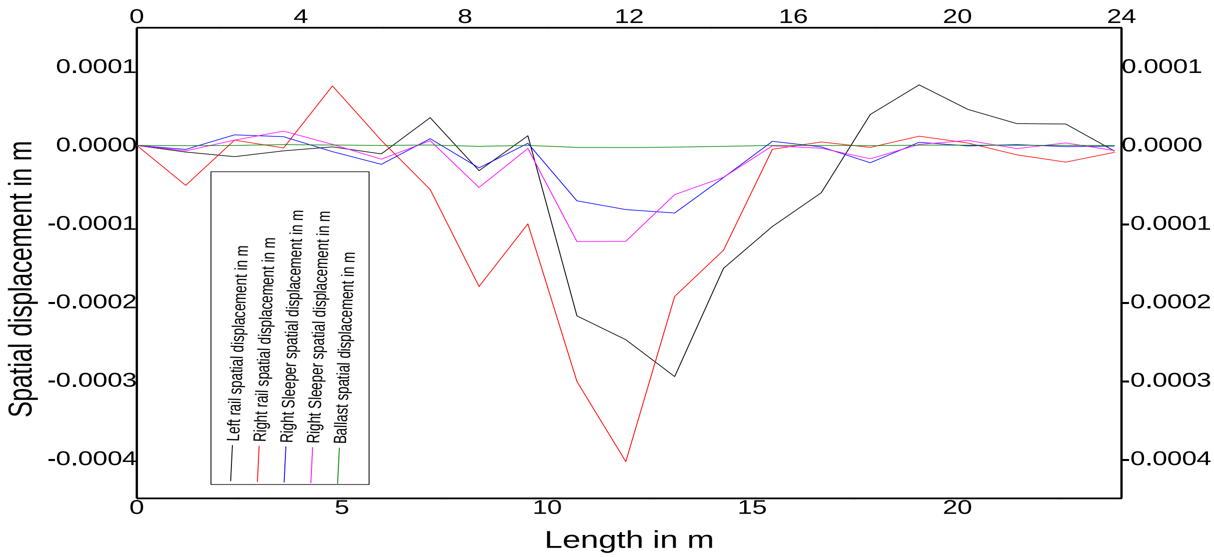

Figure 4.19 As the spatial displacement of rail, sleeper and ballast as the vehicle moves from right to the left

As we can see from the above diagram that when the wheel vehicle starts rolling on the rail from right to the left direction, the spatial displacement of the right rail becomes higher for the first half length and then the left rail will take the dominancy. Similarly, the spatial displacement of the right sleeper is higher for the first half length and then the left sleeper will be higher. In connection with this, comparing the results of spatial displacement of the rail, sleeper and ballast, we can clearly observe that the spatial displacement is maximum for the rail and minimum for the ballast.

This indicates that, as the train vehicle starts rolling on the rail, the train load is higher at the top parts of the railway track and most of this train loads will be absorbed by the rail and the remaining loads will be distributed to the sleeper and ballast.

In connection with this, what happens if the direction of the movement of the wheel is reversed? In this regards, as the vehicle moves in the reverse direction that means from the left direction to the right direction, the spatial displacement of the left rail is higher for the first half length and then the right rail spatial displacement will be higher.

In similar ways, the spatial displacement of the left sleeper is higher than the right sleeper for the first half length and then the spatial displacement of the right sleeper will be higher.

Furthermore, even though the shape of the spatial displacement of the rail, sleeper and ballast is similar for the wheel movement rolling on the rail in both directions, its magnitude is differ especially at the midway of the length or around the jointed rail.

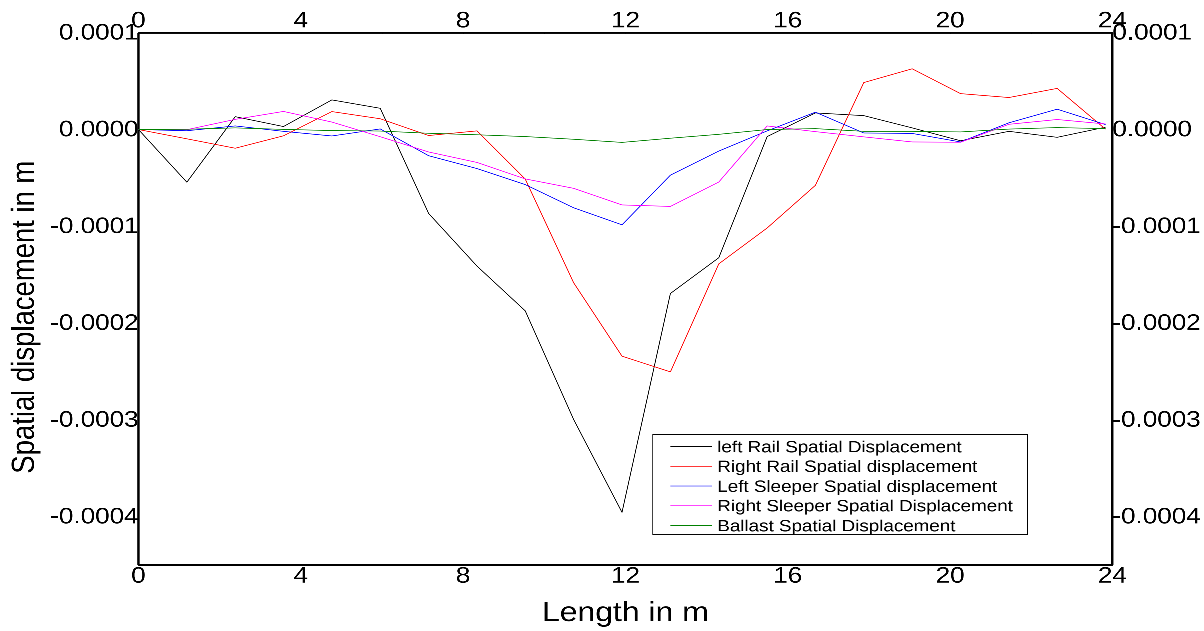

Figure 4.20 the spatial displacement of rail, sleeper and ballast as the vehicle moves from the left to the right direction

2. <u>Effect rail pad stiffness</u>

The stiffness or softness of the rail pads have an important role in reducing and increasing of the dynamic effect on the railway track structure.

➢ **Rail**

As it is clearly seen from the figure 4.21 and 4.22 that, the spatial displacement of both rails placed to the right and left side of rail joint is higher for the rail pad stiffness of 50MN/m and lower for the rail pad stiffness of 500MN/m. In connection with this, especially at the middle of the rail length or at the placement of jointed rail, the spatial displacement of rail is higher for the soften rail pad stiffness and lower for the stiffen rail pads stiffness. Thus, by introducing the stiffer rail pads stiffness, the dynamic spatial displacement of the rail can be minimized.

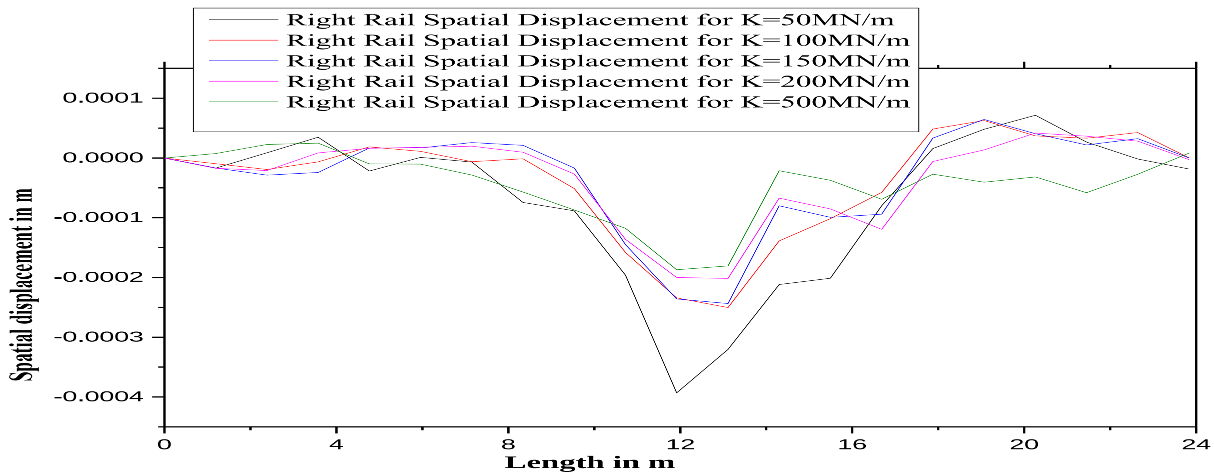

Figure 4.21 Right side jointed rail spatial displacement

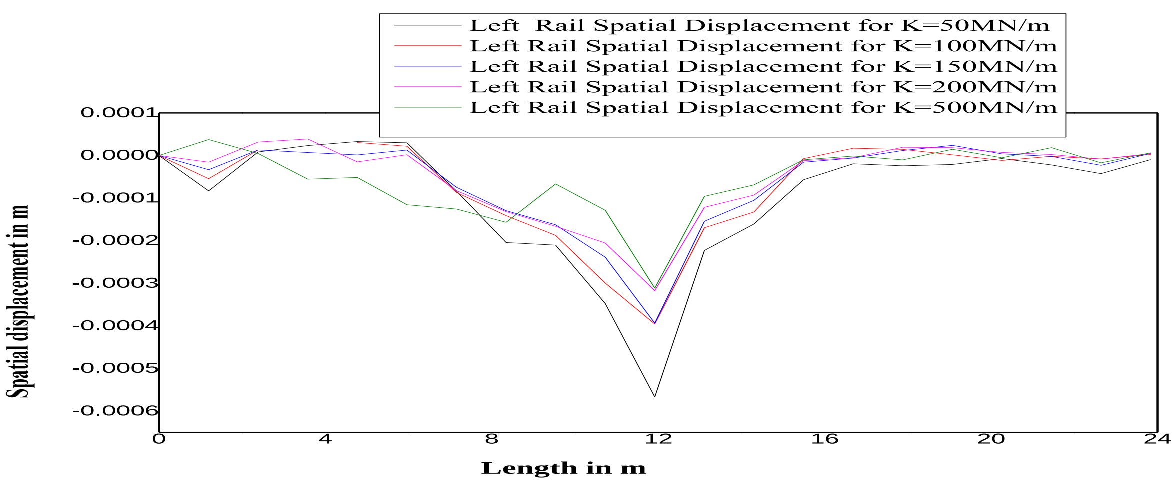

Figure 4.22 left side jointed rail spatial displacement

- **Sleeper**

As it is clearly seen from the figure 4.23 and 4.24 that, the dynamic spatial displacement of the sleeper having 50MN/m [soften rail pads stiffness] move in the upward direction at the nearly beginning of the movement of the vehicle. Comparing the result of the dynamic spatial displacement of the sleeper with the rail, it is clearly seen that introducing of stiffer rail pads stiffness have not any contribution in reducing the dynamic spatial displacement of the sleeper due to the stiffer rail pads stiffness creates more stresses on the sleeper and ballast. Hence, the dynamic spatial displacement of the sleeper is high for the stiffer rails pads stiffness. Hence, stiffening the rails pads stiffness is not more advantageous for the sleeper in reducing dynamic spatial displacement of the sleeper. However, it is more advantageous for the rail in reducing its dynamic spatial displacement of the rail.

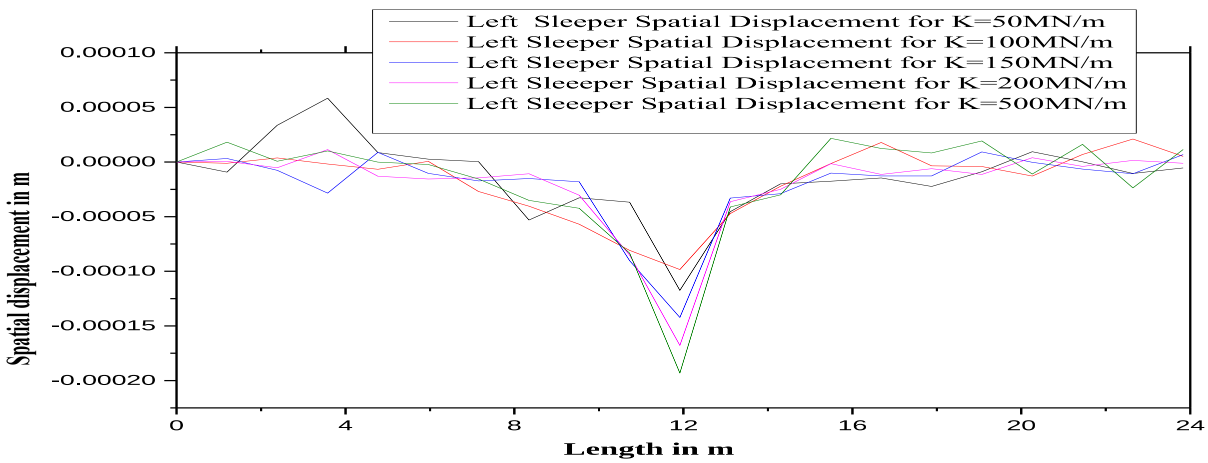

Figure 4.23 Left side of the sleeper Spatial displacement

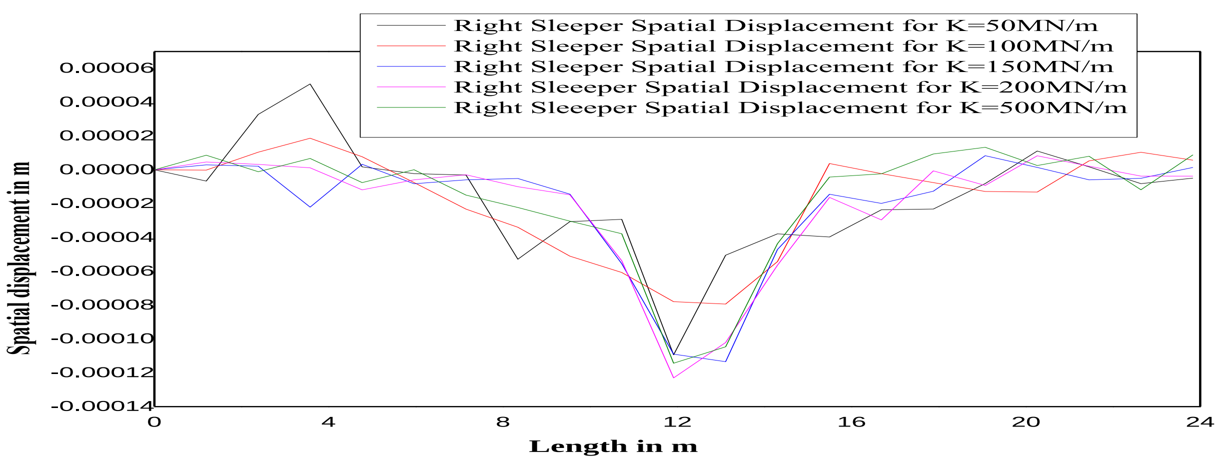

Figure 4.24 Right side of the sleeper spatial displacement

- **Ballast**

Similarly, as it is clearly seen in the figure 4.23, 4.24 and 4.25 that, the spatial displacement of the rail, sleeper and ballast is vary in zigzag forms as the rail pad stiffness is vary. Moreover, it is clearly seen in the figure 4.24 and 4.25 that, increasing rail pads stiffness from K=50MN/m to

K=500MN/m creates higher spatial displacement on the sleeper and ballast. Thus, introducing of the stiffer rail pads stiffness has not as much significant advantageous for the sleeper and ballast in reducing their dynamic spatial displacement. However, it is more advantageous for the rail in reducing its spatial displacement.

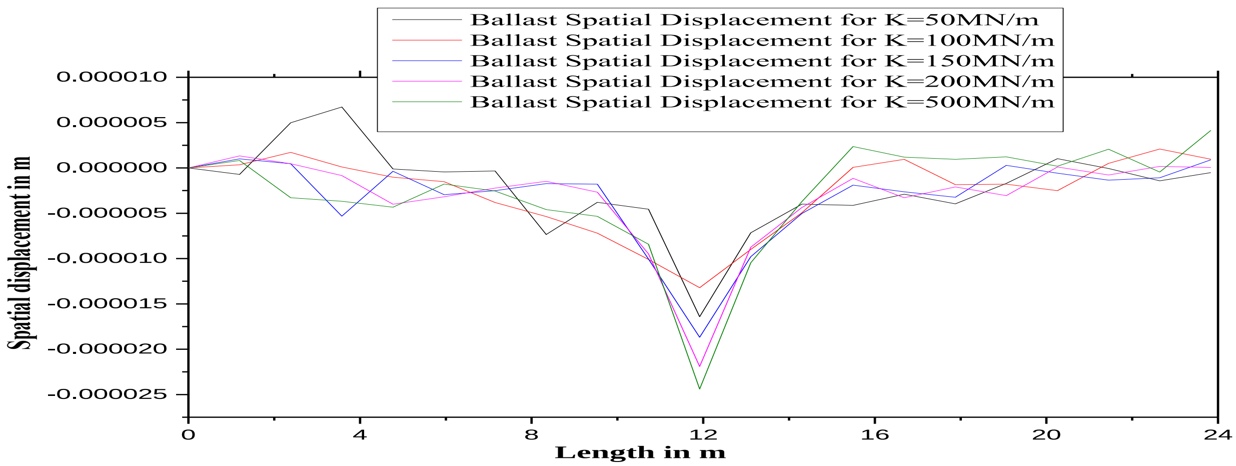

Figure 4.25 Ballast spatial displacements

Generally, we can conclude that, the spatial displacement of the rail, sleeper and ballast are maximum at the middle length of the rail or at the placement of jointed rail. Thus, it is required to minimize this maximum spatial displacement in order to reduce the dynamic effect of the jointed rail on the railway track components. Thus, this maximum spatial displacement of the rail can be minimized by introducing stiffer rail pads stiffness and maximized by introducing soften rail pads stiffness. However, the stiffer rail pads stiffness is not more advantageous for the sleeper and ballast in reducing their spatial displacement. Rather, increasing sleeper and ballast materials properties is more advantageous for minimizing their spatial displacement than stiffening of rail pads stiffness.

3. Position of the sleeper

Depending on the position of the sleeper, the placement of the jointed rail has an effect on the railway track components. In this thesis, the dynamic effect of jointed rail on the railway track components has been analyzed in the Abaqus software modeling depending on the position of the sleepers [whether it is placed between the sleepers (as suspended sleeper) or placed on the sleeper (as supported sleeper)].

- **Rail**

The dynamic spatial displacement of the rail can be varied depending on the position of the joint rail whether it is placed between the sleepers (suspended sleeper) or on the sleeper (supported sleeper). It is known that placing of the jointed rail on the supported sleeper create high impact forces on the sleeper and ballast due to the support or sleeper under the jointed rail is highly strong and stiffened than the suspended sleeper and this will create high dynamic impact forces and this will produce discomfort for the passenger even if the spatial displacement of the rail is smaller for the supported sleeper and higher for suspended sleeper see figure 4.26. Thus, placing of the rail joint between the sleepers is more practicable than placing the rail joints on the sleeper for the reason of the supported sleeper producing a discomfort for the passenger.

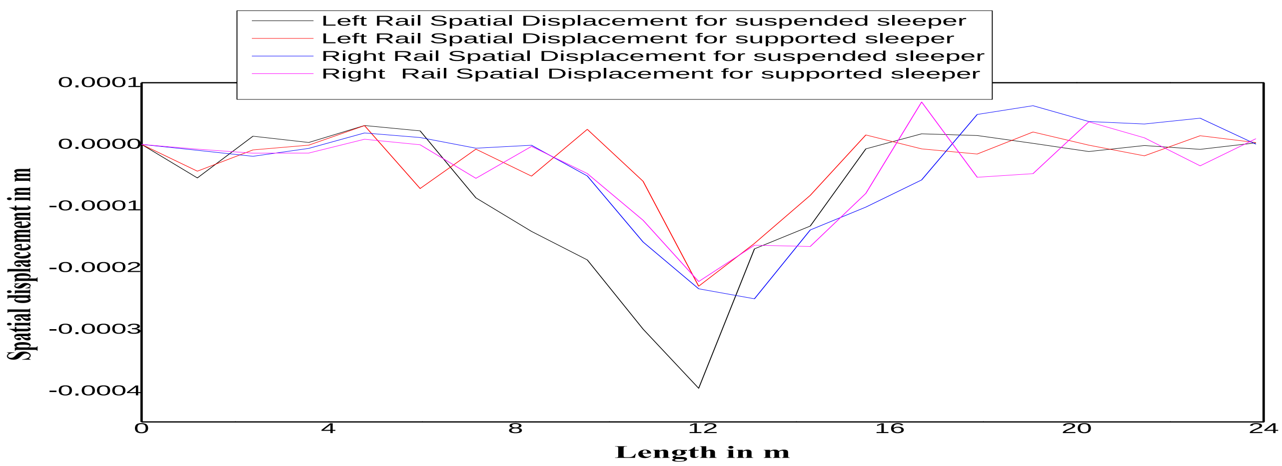

Figure 4.26 Rail spatial displacement

- **Sleeper**

It is known that supported sleeper produce higher impact forces on the train and more stresses on the sleeper and ballast and this stresses and impact forces produced on the sleeper will create higher spatial displacement on the sleeper and ballast see figure 4.27.

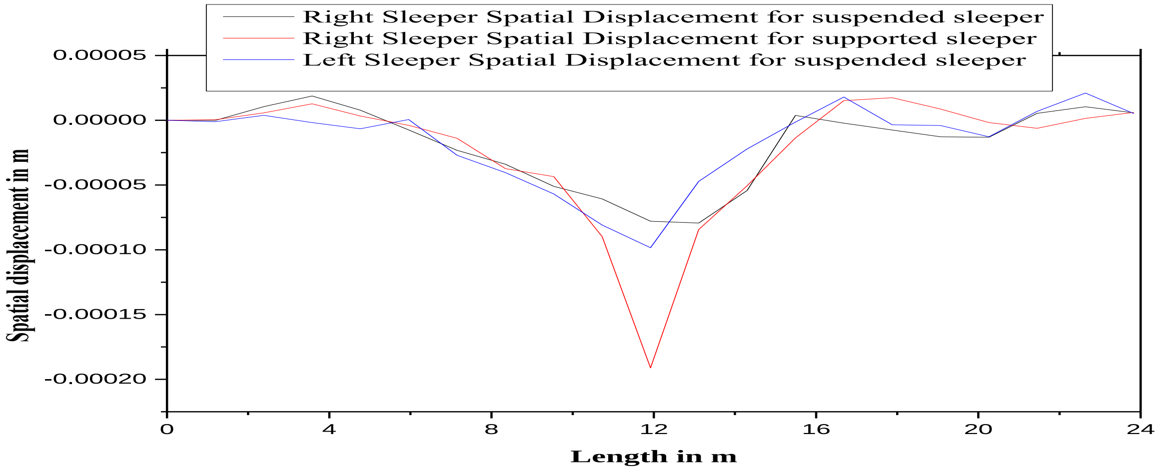

Figure 4.27 Suspended and Suppported Sleeper spatial displacement

- **Ballast**

It is known that placing of jointed rail on the sleeper creates greater impact forces and more stresses on the sleeper and ballast and this impact forces creates higher spatial displacement on the sleeper and ballast. However, placing of jointed rail between the sleepers doesn't create greater impact forces and more stress on the sleeper and ballast as the supported sleeper.

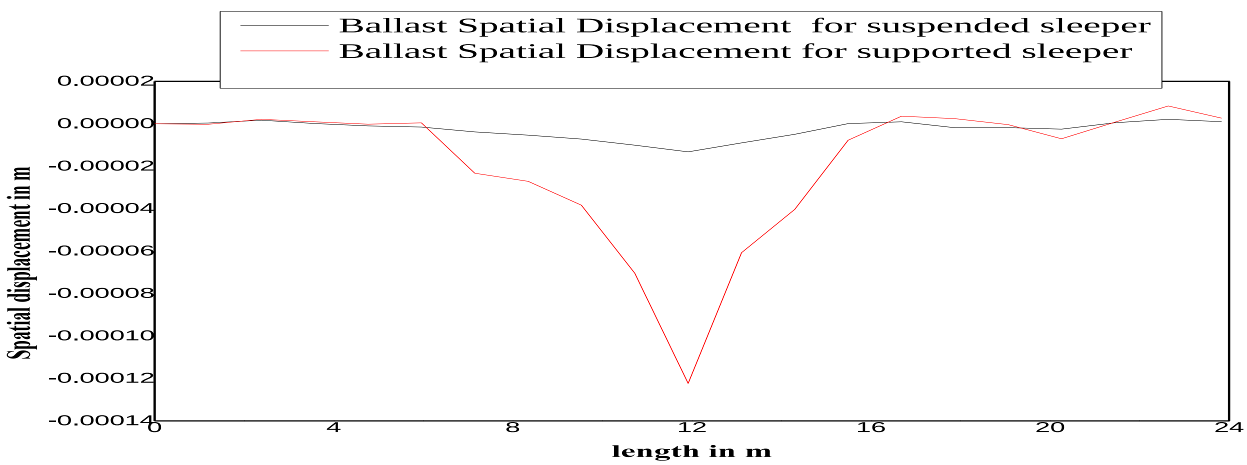

Figure 4.28 Suspended and Supported ballast spatial displacement

As it is clearly seen from the above section that, placing of the jointed rail on the sleeper creates higher dynamic impact force and stresses on the sleeper and ballast and this will generates discomfort for passengers even if the spatial displacement of the rail is minimized. Consequently, for the reason of the impact forces and stresses produced by the suspended sleeper on the sleeper and ballast is less than supported sleeper. That is why the suspended sleeper is becoming practicable throughout the world.

4. Effect of wheel number

It is common in the ABAQUS modeling, representing of the vehicle body as one wheel by introducing all the vehicle behavior on a single wheel. However, in the real world, train vehicle has multitude wheels. Thus, multitude wheel has been introduced in the Abaqus modeling to further analysis the dynamic effect of the wheel on the rail way track components,.

➢ **Rail**

It is clearly seen from figure 4.29 and 4.30 that, modeling of the track structure using single, double or triple wheels has greater effect on the dynamic spatial displacement of the railway track components. As the wheel number changes from single to triple wheel, the spatial displacement of the rail is also changed. Hence, the main aim this thesis is only to show the dynamic effect of the number of wheel in the Abaqus modeling. Accordingly, the result indicates that, modeling of the wheel using single or multitude wheel makes difference on the result. Thus, the upcoming researchers can further study the dynamic effect of the jointed rail on the railway track components by using multitude wheel to obtain the practicable result.

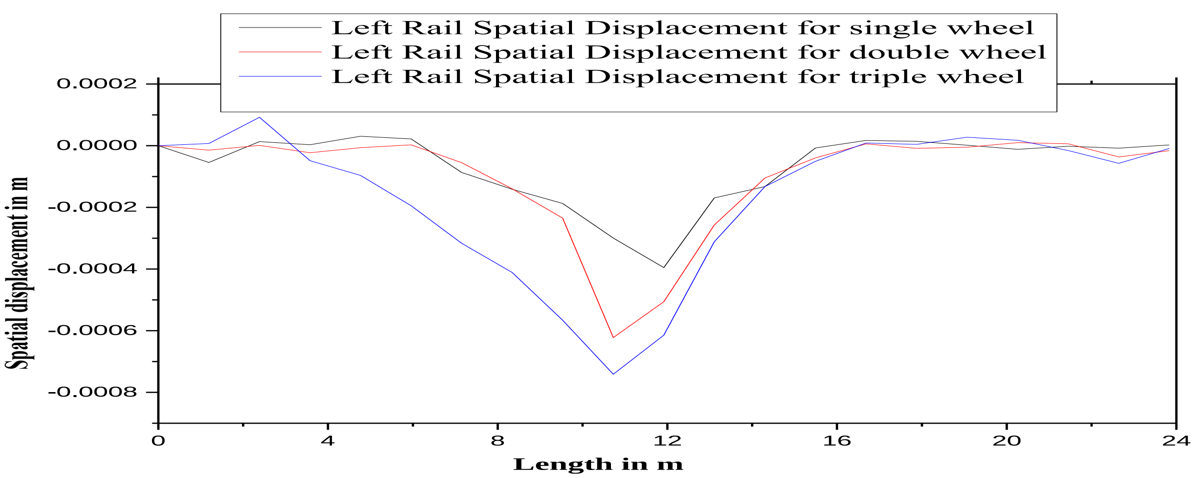

Figure 4.29 left rail spatial displacement for different number of wheel

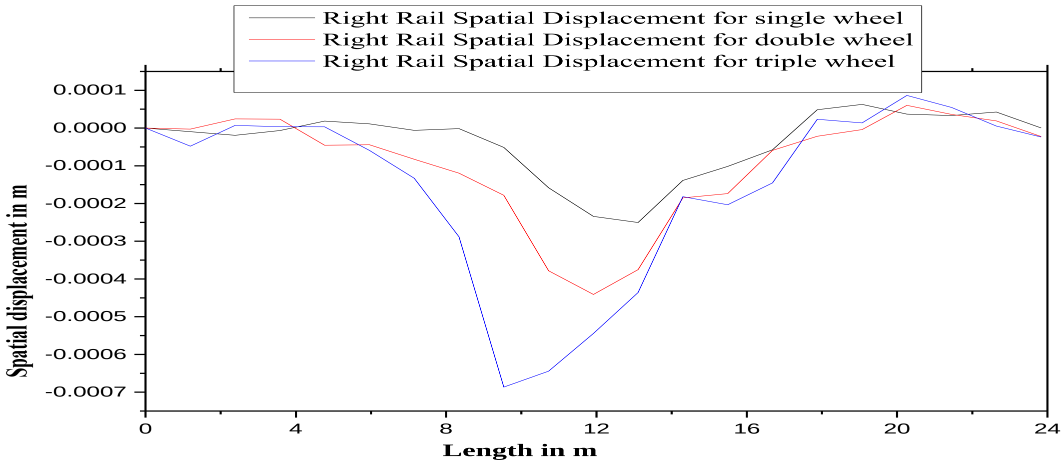

Figure 4.30 Right rail spatial displacements for different number of wheel

- **Sleeper**

The spatial displacement of the sleeper has also a similar behavior with the above rail behavior. We can clearly understand from the figure 4.31 and 4.32 that, as the number of the wheel modeling is increases, the spatial displacement of the sleeper is also increases.

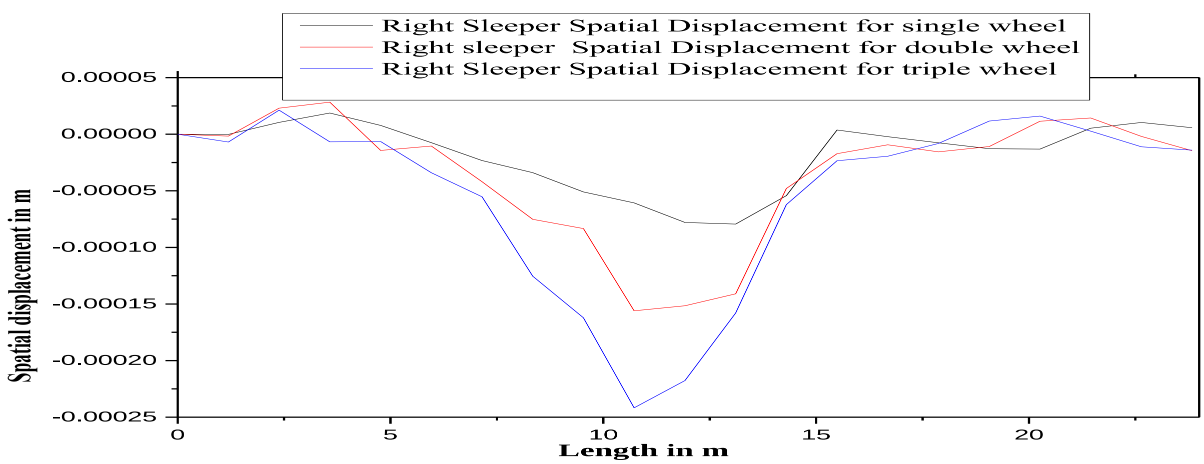

Figure 4.31 Right sleeper spatial displacement

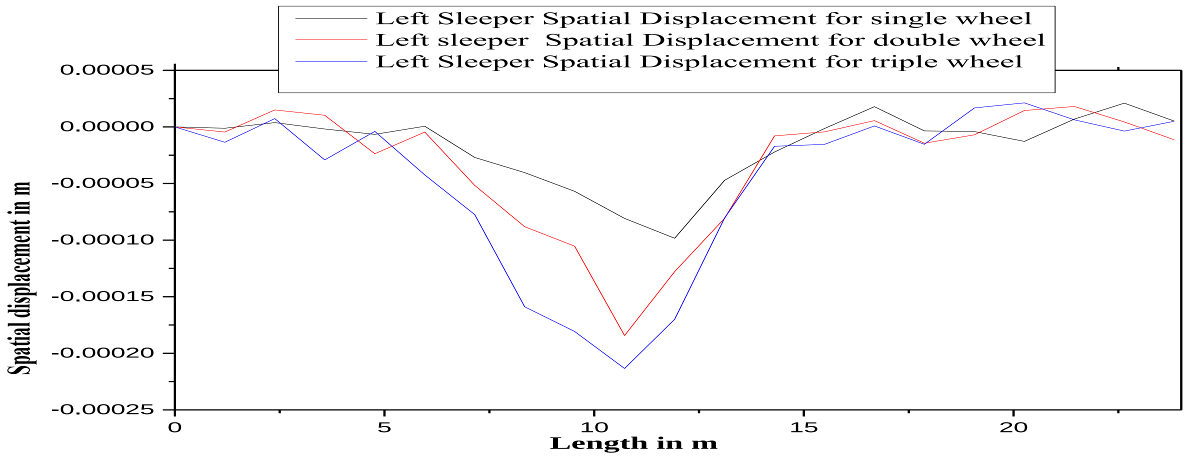

Figure 4.32 left sleeper spatial displacement

- **Ballast**

As the number of the wheel increases from single to triple, the spatial displacement of the ballast is also increases.

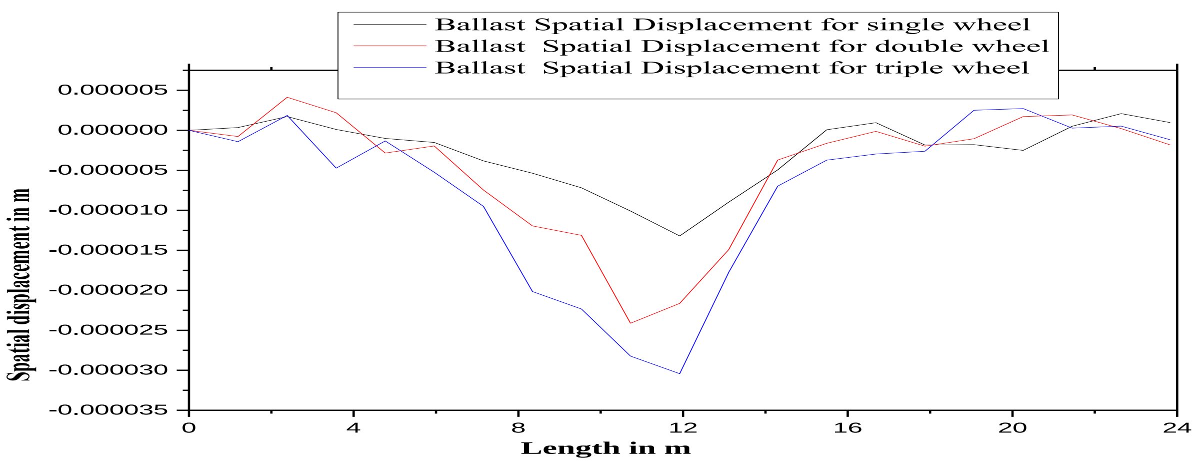

Figure 4.33 Ballast spatial displacement

From the above section, we can conclude that, the dynamic effect of the jointed rail can be affected by the vehicle characteristics of the train wheel. Thus, the models show that as the number of the wheels increase, the spatial displacement of the rail, sleeper and ballast are also increase.

5. Effect of Wheel diameter

The wheel diameter has also its own effect on the dynamic effect of the rail tracks. However, increasing of wheel diameter is highly related with its carrying capacity of the axle loads. As the diameter of wheel increases, its carrying capacity of the loads is also increases. But, in this thesis to slightly study the effect of the wheel diameter only, similar the loading effect is introduced for all wheel diameters in the Abaquas Modeling.

- **Rail**

As we can see from the figure 4.34 and 4.35 that, the spatial displacement of the left rail of the track has almost irregular behavior for the length from 0m to 12m. Even though the effect of wheel diameter doesn't make as much significant effect on spatial displacement of the rail, it has significant effect at the rail joint or 12m.

In case of the rail placed at the right side of the jointed rail, the wheel radius of 0.5m has unique sinusoidal irregular patterns for the length from 14m to 24m. However, in both cases for the left and right rail, increasing the wheel diameter, increases the spatial displacement of the rails at the jointed rail or 12m.

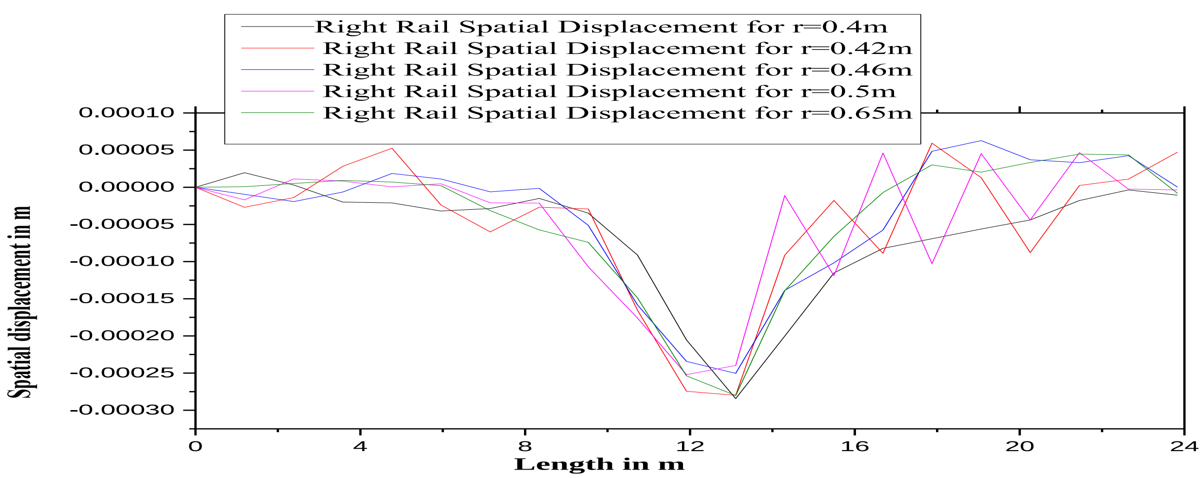

Figure 4.34 Right rail spatial displacemnt for different wheel diameter

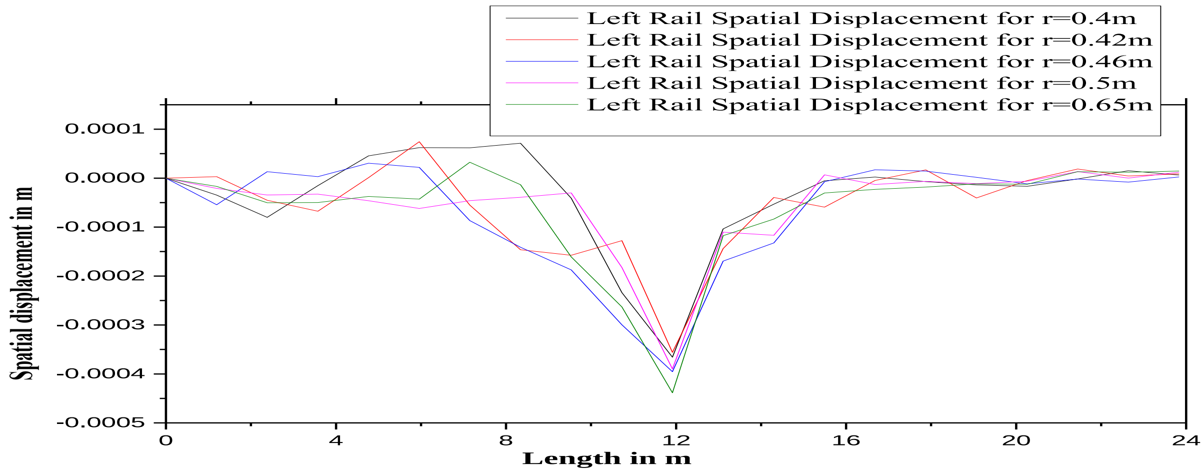

Figure 4.35 left rail spatial displacement for different wheel diameter

- **Sleeper**

It is clearly seen that the maximum spatial displacement of the sleeper is realized at the jointed rail or 12m. Further, as the radius of wheels increases from 0.4m to 0.5m, the spatial displacement of the sleeper is also increases.

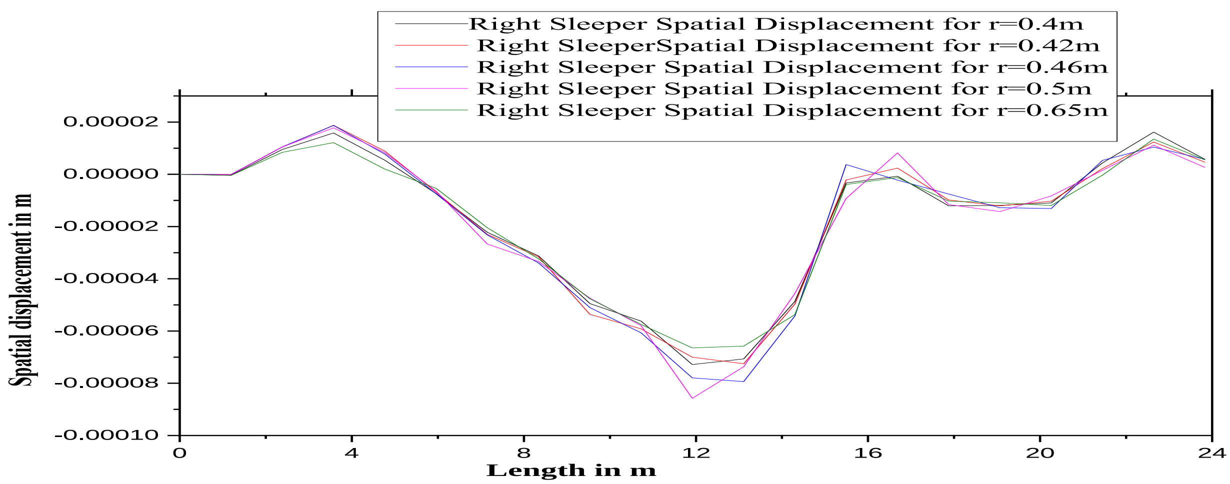

Figure 4.36 Right sleeper spatial displacement for different wheel diameter

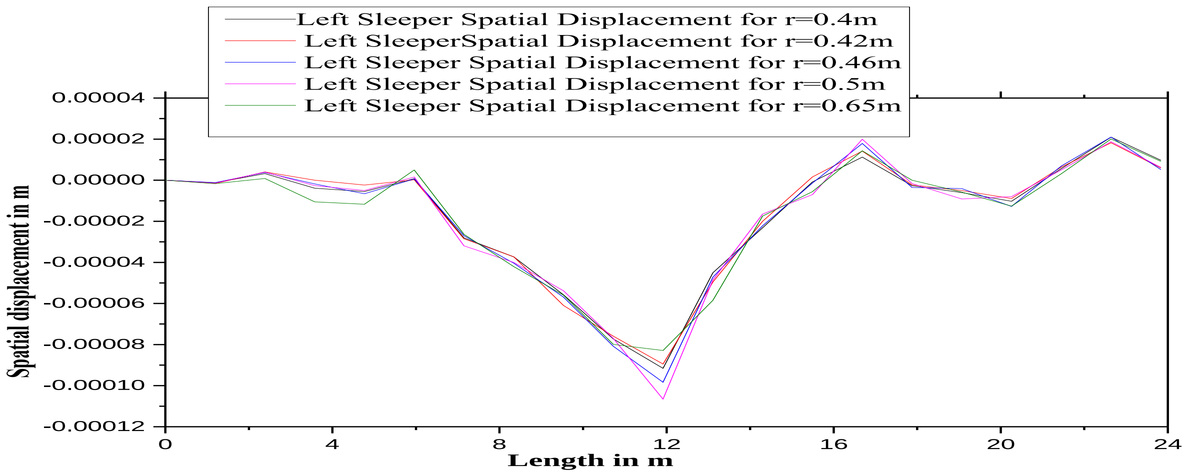

Figure 4.37 left sleeper spatial displacement for different wheel diameter

- **Ballast**

The spatial displacement of the ballast for the all-wheel diameters is similar except at the middle of the rail length or 12m. At this location, as wheel radius increases from 0.4m to 0.5m, the spatial displacement of the ballast is also increases.

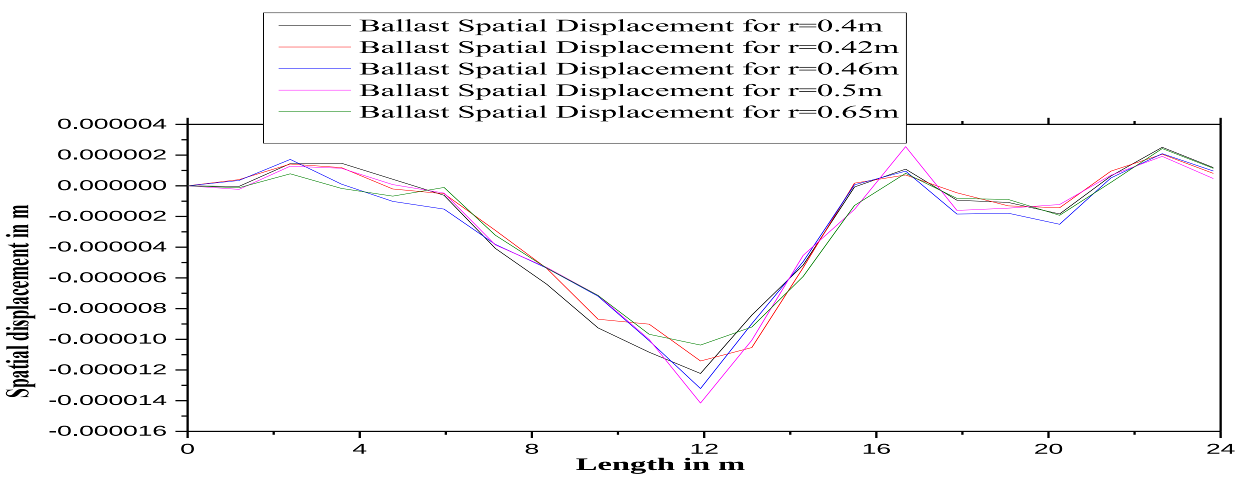

Figure 4.38 Ballast spatial displacements for different wheel diameter

Rail Joint bar Von Misses stresses

Joint bar is a plate that joins the rail together. It is obvious that as the wheel rolling over the rails, the dynamic effect of the rail especially at the jointed rail develop greater von misses stresses

As we can see from the figure 4.39 and 4.40 that, we can understand that the joint bar has maximum Von misses stresses than rail. The maximum von misses stresses developed on the joint bar is 0.12Gpa which is greater than Von Misses stresses of the rail. Therefore, special attention must be given for the design of joint bar plate especially around the bolts and plate otherwise frequent damage might occur on the joint bar.

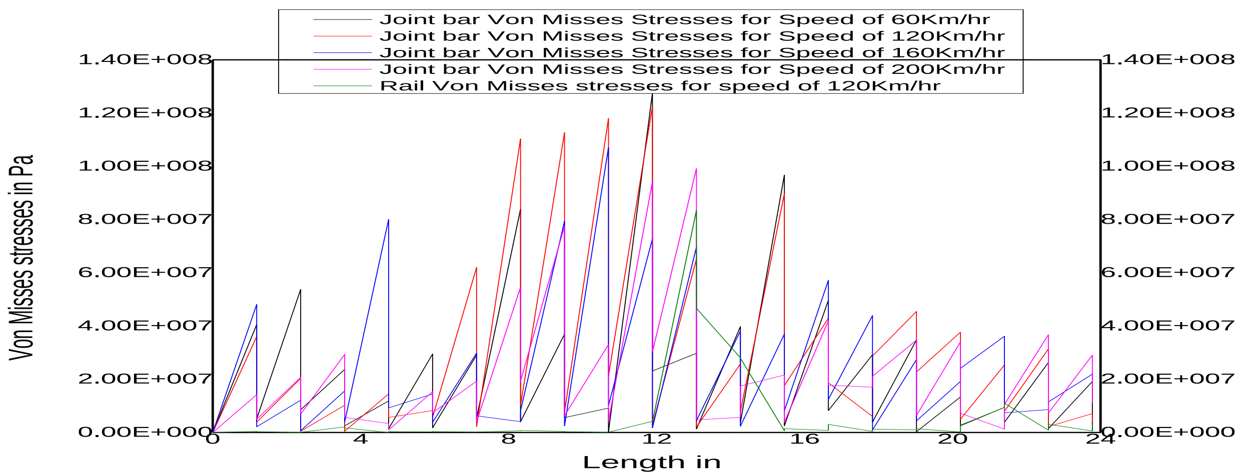

Figure 4.39 Jointed bar Von misses stresses

Effect of rail pad stiffness

The effect of Von Misses Stresses of jointed rail can be minimized by introducing different rail pads stiffness. As we can see from the figure 4.40 that, as the rail pad stiffness are increases from 50MN/m to 500MN/m, the rail Joint bar Von misses stresses is decreases. Therefore, in order to reduce the highest Von misses stresses developed at the jointed bar, it is advisable to use stiffer rail pad stiffness around the joint bar.

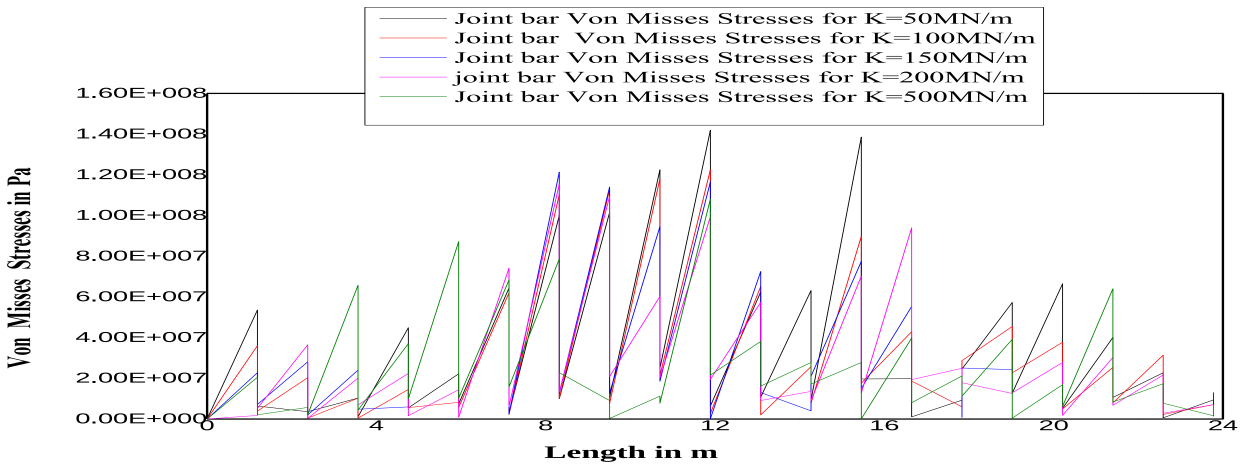

Figure 4.40 Von misses Stresses of rail pad for the vehicle speed of 120Km/hr for different rail pad stiffness

From the above section we can conclude that, the Von misses stresses developed at and around the jointed rail has greater dynamic effect on the joint bar than rail. The Von misses stress has strong relationship with the rail pad stiffness. As the rail pad stiffness are increases, the von misses stresses developed on the joint bar is decreases. In addition, the joint bar might be frequently damaged due to the maximum dynamic effect of the track developed on the joint bar plate at the jointed bar. Hence, the jointed bar must be designed in good way.

CHAPTER FIVE

CONCLUSION AND RECOMMENDATION

5.1 Conclusion

The dynamic effect of jointed rail on the railway track components at the vicinity of the jointed rail are examined and reported in this thesis. The Finite Element Method has been also used in the Abaqus modeling.

To achieve a reasonable model size which is acceptable to the available computing facility, several idealization and simplification strategies have been employed in following aspects such as jointed rail assembly and wheel profile, material modeling, boundary conditions and loading

The dynamic effect of jointed rail on railway tracks components was investigated and reported. The dynamic explicit analysis was also analyzed in the Abaqus Modeling for the jointed rail using different scenarios such as the effect of the vehicle speeds, rail pads stiffness, position of the sleepers, wheel number and diameter were investigated and reported in this thesis.

From the above FE analysis, the following conclusion was drawn.

- The vertical vibration of the rail, sleeper and ballast has variable results and magnitudes when the frequency range is differ. The results of this thesis indicates that, the vertical vibration of the rail and sleeper is maximum at the frequency range from 90Hz to 130Hz and the vertical vibration of the ballast is maximum at the frequency range from 174Hz to 300Hz. Thus, special attention shall be given for the rail and sleeper in the frequency range of 90Hz to 130Hz and for the ballast in the frequency range of 174Hz to 300Hz. In this range, increasing the rail, sleeper and ballast material strengths can minimize the spatial displacement of the same.

- As the vehicle speeds of the train increases from 60Km/hr to 200Km/hr, the spatial displacement of the rail, sleeper and ballast is also increases in zigzag forms for the entire length of the rail. In connection with this, the maximum spatial displacement of the rail, sleeper and ballast are observed at the jointed rail or at 12m.

- The spatial displacement of the rail, sleeper and ballast is advanced at the middle length of the rail or at the placement of jointed rail. Hence, this advanced spatial displacement of the rail can be minimized by introducing stiffer rail pads stiffness and maximized by introducing soften rail pads stiffness. However, the stiffer rail pads stiffness is not advantageous for the sleeper and ballast in reducing their spatial displacement. Rather, increasing sleeper and ballast materials properties is more advantageous for minimizing the sleeper and ballast spatial displacement than introducing of rail pads stiffness.

- Placing of the jointed rail on the sleeper or supported sleeper will creates higher dynamic impact force and stresses on the sleeper and ballast and this will generates discomfort for passengers. Consequently, for the reason of the impact forces and stresses produced by the suspended sleeper on the sleeper and ballast is less than the supported sleeper, the suspended sleeper is currently becoming practicable throughout the world.
- The dynamic effect of the jointed rail can be affected by the vehicle characteristics of the train wheel. Thus, the model shows that as the number of the wheels increase from single to multitude wheel, the spatial displacement of the rail, sleeper and ballast are also increase.
- As the wheel diameter increases, the spatial displacement of the rail, sleeper and ballast has almost similar patterns for the entire length of the rail except at the middle of the rail length or at the jointed rail in which the spatial displacement of the rail, sleeper and ballast is maximum at this jointed rail.
- The Von misses stresses developed at and around the jointed rail has greater dynamic effect on the joint bar than rail. The Von misses stress has strong relationship with the rail pad stiffness. As the rail pad stiffness are increases, the von misses stresses developed on the joint bar is decreases. In addition, the joint bar might be frequently damaged due to the maximum dynamic effect of the track developed on the joint bar plate at the jointed bar. Hence, the jointed bar must be designed in good way.

5.2. Recommendations

There are recommendations listed as follows which could further require improvement on the study of the effects of rail joint on the railway tracks:

(1) The dynamic analysis of rail joints has a strong relationship with vehicle components such as bogies, car bodies and so on. However, the effect of the vehicle Components on the jointed rail was not studied in this studied.

(2) In this thesis, the only FE modeling is described. The effect of this FE modeling of jointed rail could be further developed by comparing the results with the actual site experimental results.

(3) An actual train of the wheel has conic shape. However, for making of the wheel simple and less complex, the wheel was modeled as circle. Thus, it is known that, the conical shape of the wheel has an effect on the result since it is conical and it will be aggravated during the dynamic loads. Thus, it is required to analyze the dynamic effect of this conical shape of the wheel on the jointed rail and hence the upcoming researcher might investigate this effect in detail.

(4) To get reasonable and precise results, the effects of rail joints should be studied by the 3D FE modeling.

REFERENCES

[1]. Thambiratnam, D. and Y. Zhuge, Dynamic analysis of beams on an elastic foundation subjected to moving loads. Journal of Sound and Vibration, 1996. 198(2): p. 149-169.

[2]. Wang, Y., et al., Transient responses of beam with elastic foundation supports under moving wave load excitation. International Journal of Engineering and Technology, 2011. 1(2): p. 137-143.

[3]. Grassie, S.L., et al., The Dynamic Response of Railway Track to High Frequency Vertical Excitation. Journal of Mechanical Engineering Science, 1982. 24(2): p. 77-90.

[4]. Lei, X. and N.A. Noda, Analyses of dynamic response of railway track to high frequency vertical excitation. Journal of Sound and Vibration, 2002. 258(1): p. 147-165.

[5]. Zhai, W., K. Wang, and C. Cai, Fundamentals of vehicle–track coupled dynamics. Vehicle System Dynamics, 2009. 47(11): p. 1349-1376.

[6]. Lu, F., et al., Symplectic analysis of vertical random vibration for coupled vehicle–track systems. Journal of Sound and Vibration, 2008. 317(1–2): p. 236-249.

[7]. Diana, G., et al., Modelli matematici per lo studio della interazione veicolo strutturaarmamento. Ingegneria ferroviaria, 1995(12).

[8]. Zhai, W. and Z. Cai, Dynamic interaction between a lumped mass vehicle and a discretely supported continuous rail track. Computers & Structures, 1997. 63(5): p. 987-997.

[9]. Dukkipati, R.V. and R. Dong, The Dynamic Effects of Conventional Freight Car Running over a Dipped-joint. Vehicle System Dynamics, 1999. 31(2): p. 95-111.

[10] Jeffs T and Tew GP. A review of track design procedures: volume 2 - sleepers and ballast. Melbourne, Australia: Railways of Australia, 1991

[11] Mohammad Worya Khordehbinan. Investigation on the Effect of Railway Track Support System Characteristics on the Values of Track Modulus

[12] W.Zhai and Z.Cai. dynamic interaction between a lumped mass and discretely supported rail Department of Civil Engineering, Royal Military College of Canada, Kingston, Ontario, Canada K7K 5L0

[13]. Office for Research and Experiments. Question D 71: Stresses in the rails, the ballast and in the formation resulting from traffic loads. Interim report no. 1, 1965. Utrecht, The Netherlands: International Union of Railways.

[14]. Doyle NF. Railway track design: a review of current practice. Occasional paper 35, 1998. Canberra, Australia: Bureau of Transport Economics.

[15]. Broadley JR, Johnston GD and Pond B. The dynamic impact factor. In: The railway engineering conference, Sydney, Australia, 1981, pp.87–91

[16] Jeong DY. Preliminary engineering analysis of joint bar fatigue life. Volpe Center report for the Federal Railroad Administration, 2002.

[17]. Jenkins HH, Stephenson JE, Clayton GA, et al. The effect of track and vehicle parameters on wheel/rail vertical dynamic force. Railway Engng J 1974; 3: 2–16.

[18]. Talamini B, Jeong DY and Gordon J. Estimation of the fatigue life of railroad joint bars. In: The ASME/IEEE joint rail conference & internal combustion engine spring technical conference, Pueblo, CO, United States: Federal Railroad Administration, 13–16 March 2007, pp.1–10.

[19]. COENRAAD ESVELD, Modern Railway Track, 2nd edition, TU Delft University of Technology, 2001

[20] C. Gonzalez-Nicieza, M. Alvarez-Fernandez, A. Menendez-Diaz, A. Alvarez-Vigil, and F. Ariznavarreta- Fernandez, Failure analysis of concrete sleepers in heavy haul railway tracks, Eng. Failure Anal. 15 (2008), pp. 90–117.

[21] D. Thambiratnam andY. Zhuge, Finite element analysis of track structures, Microcomput. Civil Eng. 8 (1993), pp. 467–476.

[22] T. Telliskivi and U. Olofsson, Wheel–rail wear simulation, Wear 256(7–8) (2004), pp. 817 831.

[23] Akke Simon Johanna SUIKER The mechanical behavior of ballasted tracks, ter verkrijging van de graad van doctor aan de Technische Universiteit Delft, op gezag van de Rector Magnificus prof. dr. ir. J.T. Fokkema, in het openbaar te verdedigen ten overstaan van een commissie, door het College voor Promoties aangewezen, op maandag 24 juni 2002 te 16:00 uur.

[24] Tore Dahlberg Railway track settlement-a literature review Division of Solid Mechanics, IKP, Linköping University, SE-58183 Linköping, Sweden.

[25] M J M M Steenbergen_ and C Esveld. Rail weld geometry and assessment concept, , Railway Engineering, Faculty of Civil Engineering and Geosciences, Delft University of Technology, Delft, The Netherlands Delft, 22 February 2006.DOI: 10.1243/09544097JRRT38.

[26] Zhang, Y. J., Murray, M. H. and Ferreira. L. (2000). Modeling Rail Track Performance: An Integrated Approach. , *Transport Journal*, 187-194.

[27]. ABAQUS Online Documentation: Version 6.9 (2011). http://abqdoc.byv.kth.se:2011/v6.9/

[28] CAO CHANGYONG et al, Dynamic Analysis of Bernoulli–Euler Beam on Two-Parameter Foundation Subjected to Moving Harmonic Load, Dalian University of Technology, Dalian, P. R. China.

[29] Prof.dr.ir. COENRAAD ESVELD, Track Structures in an Urban Environment, TU Delft, 1997

[30] Berggren, E.G., Li, M.X.D., Spännar, J., 2006, A new approach to the analysis and presentation of vertical track geometry quality and rail roughness with focus on train-track interaction and wavelength content. *Proc. 7th Int. Congress on Contact Mechanics and Wear of Rail/Wheel systems CM 2006*, Brisbane, Australia

[31]. E. Thorenfeldt, A. Tomaszewicz, J.J. Jensen, 1987: "Mechanical properties of high-strength concrete and application in design," Proceedings of the Symposium "Utilization of High Strength Concrete," Stavanger, Norway, pp. 149-159.

[32] Q. Feng, X. Lei, S. Lian, 2010: "Ground vibration generated by high-speed train," Proceedings of International Conference on Railway Engineering, Beijing, pp. 379-384

[33] Michaël Jozef Matthatias Maria STEENBERGEN June 2008, Wheel-rail interaction at short-wave irregularities

[34] Newton, S.G., Clark, R.A., 1979. An investigation into the dynamic effects on the track of wheel flats on railway wagon. J. Mech. Eng. Sci. 21(4), 287–297.

[35] Akke Simon Johanna 2002

[36] Johnson, 1985

APPENDIX

```
*Heading
** Job name: Job-jointed rail Model name: Model-1
** Generated by: Abaqus/CAE 6.12-1
*Preprint, echo=NO, model=NO, history=NO,
**
** PARTS
**
*Part, name=ballast
*Element, type=CPS4R
8000, 8799, 8800, 8811, 8810
** Section: ballast
*Solid Section, elset=Set-1, material=ballast
,
*End Part
**
*Part, name=bogie
*Node
*Element, type=R2D2
*Element, type=MASS, elset=Set-1_Inertia-1_MASS_
23, 23
*Mass, elset=Set-1_Inertia-1_MASS_
62000.,
*Element, type=ROTARYI, elset=Set-1_Inertia-1_ROTI_
24, 23
```

```
*Rotary Inertia, elset=Set-1_Inertia-1_ROTI_
0., 0., 619083., 0., 0., 0.
*End Part
**
*Part, name="rail joint bar"
*Node
*Element, type=B21
** Section: rail joint bar  Profile: rail joint bar
*Beam Section, elset=Set-1, material=steel, temperature=GRADIENTS, section=RECT
0.034, 0.087
0.,0.,-1.
*End Part
**
*Part, name=rail1
*Element, type=B21

** Section: rail  Profile: rail
*Beam Section, elset=Set-1, material=steel, temperature=GRADIENTS, section=I
0.07401, 0.17, 0.146, 0.07, 0.028, 0.049, 0.0165
0.,0.,-1.
*End Part
**
*Part, name=rail2
*Element, type=B21
** Section: rail  Profile: rail
```

*Beam Section, elset=Set-1, material=steel, temperature=GRADIENTS, section=I

0.07401, 0.17, 0.146, 0.07, 0.028, 0.049, 0.0165

0.,0.,-1.

*End Part

**

*Part, name=sleeper

*Element, type=B21

** Section: sleeper Profile: sleeper

*Beam Section, elset=Set-1, material="sleeper concrete", temperature=GRADIENTS, section=RECT

1.3, 0.18

0.,0.,-1.

*End Part

**

*Part, name=wheel

*Element, type=R2D2

*Mass, elset=Set-1_Inertia-1_

500.,

*End Part

**

** Constraint: Constraint-1

*Rigid Body, ref node=_PickedSet245, elset=b_Set-98

** Constraint: Constraint-2

*Rigid Body, ref node=_PickedSet260, elset=b_Set-109

** Constraint: Constraint-3

```
*Coupling, constraint name=Constraint-3, ref node=m_Set-123, surface=s_Set-123_CNS_
*Kinematic
** Constraint: Constraint-4
*Coupling, constraint name=Constraint-4, ref node=m_Set-125, surface=s_Set-125_CNS_
*Kinematic
** Constraint: Constraint-5
*Coupling, constraint name=Constraint-5, ref node=m_Set-127, surface=s_Set-127_CNS_
*Kinematic
** Constraint: Constraint-6
*Coupling, constraint name=Constraint-6, ref node=m_Set-129, surface=s_Set-129_CNS_
*Kinematic
*Spring, elset=Springs/Dashpots-rail and sleeper-spring
1e+08
*Dashpot, elset=Springs/Dashpots-rail and sleeper-dashpot
15000.
*Spring, elset=Springs/Dashpots-bogie-spring
1.834e+06
*Dashpot, elset=Springs/Dashpots-bogie-dashpot
7500.
** MATERIALS
*Material, name=ballast
*Density
1600.,
*Drucker Prager
45., 0.8, 15.
```

```
*Drucker Prager Hardening
400000.,0.
*Elastic
 2.1e+08, 0.3
*Material, name="sleeper concrete"
*Density
2500.,
*Elastic
 3.5e+10, 0.22
*Material, name=steel
*Density
7800.,
*Elastic
 2.1e+11, 0.3
** INTERACTION PROPERTIES
*Surface Interaction, name=IntProp- between wheel and rail
*Friction
 0.3,
*Surface Behavior, pressure-overclosure=HARD
*Surface Interaction, name=IntProp-between sleeper and ballast
*Friction
30.,
*Surface Behavior, no separation, pressure-overclosure=HARD
** ----------------------------------------------------------------
**
```

```
** STEP: Step-1
**
*Step, name=Step-1
*Dynamic, Explicit
, 0.715
*Bulk Viscosity
0.06, 1.2
**
** BOUNDARY CONDITIONS
**
** Name: BC-1 Type: Displacement/Rotation
*Boundary
Set-100, 1, 1
Set-100, 6, 6
** Name: BC-2 Type: Displacement/Rotation
*Boundary
Set-101, 1, 1
Set-101, 6, 6
** Name: BC-3 Type: Displacement/Rotation
*Boundary
Set-5, 1, 1
Set-5, 6, 6
** Name: BC-4 Type: Displacement/Rotation
*Boundary
sleeper-1.Set-1, 1, 1
```

```
sleeper-1.Set-1, 6, 6
** Name: BC-5 Type: Displacement/Rotation
*Boundary
"top ballast", 1, 1
"top ballast", 6, 6
** Name: BC-6 Type: Displacement/Rotation
*Boundary
Set-104, 1, 1
Set-104, 2, 2
Set-104, 6, 6
** Name: BC-7 Type: Velocity/Angular velocity
*Boundary, type=VELOCITY
Set-113, 1, 1, 33.33
Set-113, 6, 6, 72.46
**
** LOADS
**
** Name: Load-1   Type: Concentrated force
*Cload
Set-106, 2, -125000.
**
** INTERACTIONS
**
** Interaction: Int-1
*Contact Pair, interaction=IntProp-1, mechanical constraint=PENALTY, cpset=Int-1
```

m_Surf-1, s_Surf-1

** Interaction: Int-2

*Contact Pair, interaction=IntProp-1, mechanical constraint=PENALTY, cpset=Int-2

m_Surf-1, s_Surf-3

** Interaction: Int-3

*Contact Pair, interaction=IntProp-2, mechanical constraint=PENALTY, cpset=Int-3

m_Surf-4, s_Surf-4

**

** OUTPUT REQUESTS

**

*Restart, write, number interval=1, time marks=NO

**

** FIELD OUTPUT: F-Output-1

**

*Output, field

*Node Output

A, RF, U, V

*Element Output, directions=YES

EVF, MISES, MISESMAX, S, SVAVG

*Contact Output

CFORCE, CSTRESS

**

** HISTORY OUTPUT: H-Output-1

**

*Output, history, variable=PRESELECT

** FIELD OUTPUT: F-Output-1

**

*Output, field, frequency=1

*Node Output

CF, RF, U

*Element Output, directions=YES

LE, PE, PEEQ, PEMAG, S

*Contact Output

CDISP, CFORCE, CSTRESS

**

** HISTORY OUTPUT: H-Output-1

**

*Output, history, variable=PRESELECT, frequency=1

*End Step